method (*19*) using $CHCl_3$-0.1 M HCl in methanol-1 M $MgCl_2$ (pH 2) (1 : 2 : 0.8, v/v) as a solvent.

Neutral-acidic fractional extraction of PIP

[^{14}C]PIP was sufficiently extracted using the Bligh and Dyer method (*19*) with an acidic solvent from PIP-synthase reaction mixture, but not extracted using a neutral solvent (neutral extraction; Supplementary Table SI). Therefore, PIP could be separated from the other lipids containing PI by this newly devised fractional-extraction method. The reaction mixture was first extracted using the neutral extraction. PIP was recovered from the acidified remainder (the upper aqueous layer and fluff) into a chloroform fraction.

Thin-layer chromatography

Thin-layer chromatography (TLC) of lipids was performed on a Silica Gel 60 plate (Merck, Tokyo, Japan) with the following solvent: chloroform, methanol, acetic acid and water (80 : 30 : 20 : 10). Phospholipid spots were visualized by spraying acid molybdate reagent. Radioactive spots on the TLC plate were recorded using a Fujifilm FLA-5000 fluor-image analyser with an imaging plate (Fujifilm type BAS-MS for ^{14}C material or BAS-TR for ^{3}H material, Fujifilm, Japan).

Fast atom bombardment-mass spectrometry of the PIP-synthase reaction products (PIP and PI)

To obtain the PIP-synthase reaction products in an amount large enough for structural analysis, the volume of the reaction mixture was increased 20 times (concentration of the reactants was not changed) and the incubation time was prolonged to 4 h. PIP (dioleoyl) was obtained by neutral–acidic fractional extraction because PIP (dioleoyl) was unstable during the recovery from silica gel scraped from the TLC plate. The purified PIP was converted to PI (dioleoyl) by incubating with *M. smegmatis* cell walls containing PIP dephosphorylation activity and purified by TLC. The PI (dioleoyl) scraped from TLC plates was extracted using a neutral solvent. The thus obtained PIP and PI were analysed by fast atom bombardment-mass spectrometry (FAB-MS) using a mass spectrometer (JEOL JMS DX-303) with a glycerol matrix in negative mode.

Analytical methods

Phosphate (*20*) and protein (*21*) were determined as described earlier. Radioactivity was counted using a liquid scintillation spectrometer (Aloka LSC-3500E, Japan) with Aquasol-2 (Packard, Meriden, CT, USA) as the scintillation cocktail.

Construction of the expression plasmids for the PIP synthase genes of mycobacteria

Nucleic acid sequences of genes coding for the putative PIP synthases of *Mycobacterium* species (protein id: *M. smegmatis* mc^2 155, ABK73364.1; *M. bovis* BCG, CAL72625.1; *M. marinum* M, ACC40540.1; and *M. abscessus*, CAM62975.1) were obtained from Genome Information Broker (http://gib.genes.nig.ac.jp/). The putative PIP synthases were searched by using FASTA3 search tool and the amino acid sequence of AIP synthase (protein id: AAB86163.1) of *M. thermautotrophicus* as a query. The putative PIP-synthase genes of the mycobacteria were amplified by polymerase chain reaction (PCR) directly from the genomic DNAs of each species. The genomic DNAs of mycobacteria were extracted from the cells suspended in distilled water by boiling for 5 min. After centrifugation (15,000 r.p.m. for 5 min), the supernatants were used as template for PCR. The following primer sequences were used: *M. smegmatis* mc^2 155 forward, 5′-GACGGAAAAGCGCCCACCATATGAGCAATG-3′; reverse, 5′-CTGCCCGCCGAGCGGGATGCGTCGACAAAG-3′; *M. bovis* BCG forward, 5′-ACCGAGTGGGCTCGGCACATATGAGCA AGC-3′; reverse, 5′-AGCTTCAAGCCCTTAAGGTCGACAATC ACC-3′; *M. marinum* forward, 5′-GCACATATGAGCAAGGCGC CCTTCTTGTCC-3′; reverse, 5′-GCCGGGGTCGACATCACC GCTGCGTCTTTC-3′; *M. abscessus* forward, 5′-CACCGCCTGG GAGCAGTTCATATGAG CGGC-3′; reverse, 5′-GGCGCGCTCT CCGTCGACACTCATGGCTGA-3′. The restriction enzyme (*Nde*I for forward primer and *Sal*I for reverse primer) recognition sites are underlined. The amplified genes were cloned with a TOPO TA Cloning kit (Invitrogen, Carlsbad, CA, USA) according to the manufacturer's instructions. Transformation was performed with competent *E. coli* TOP10 cells provided by the manufacturer. The genes inserted into the pCR2.1-TOPO vector were digested by restriction enzymes *Nde*I and *Sal*I. After confirming the fragment sizes by gel electrophoresis with a 1.5% agarose gel, the fragments were extracted and purified using GenElute^{TM} Minus EtBr Spin Columns (Sigma-Aldrich, St Louis, MO, USA). The purified fragments were inserted into the corresponding sites of the expression vector, pET21a (Merck Ltd). The presence of the appropriate inserts was confirmed by DNA sequencing. Expression vectors were designated pET21a-smeg-PIPS (PIP synthase of *M. smegmatis* mc^2 155), pET21a-BCG-PIPS (PIP synthase of *M. bovis* BCG), pET21a-mari-PIPS (PIP synthase of *M. marinum*) and pET21a-abs-PIPS (PIP synthase of *M. abscessus*), respectively. The expression vectors were chemically inserted into the expression host cell line BL21(DE3).

Expression of PIP synthase in E. coli

To confirm that the cloned genes from *Mycobacterium* species really encoded PIP synthase, *E. coli* BL21-(Merck Ltd) carrying pET21a-PIPS were grown in Luria Bertani medium containing 50 μg/ml ampicillin. PIPS gene expression was induced by adding isopropyl β-D-thiogalactopyranoside (1 mM) for 3 h. The membrane fraction of the sonicator-disrupted cells in 0.1 M Bicine buffer (pH 8.0) containing 10 mM 2-mercaptoethanol were used for PIP synthase measurements.

Anion-exchange chromatography

To detect inositol and inositol phosphate in the reaction mixture of free inositol incorporation into lipid, the aqueous fraction was fractionated with a 1-ml column of Dowex-1 (X8; formate form). Inositol and inositol phosphate were eluted with water and 0.1 M formic acid/0.2 M ammonium formate, respectively (*22*).

Results

Activity of PIP synthase and PIP phosphatase

When CDP-DAG(dioleoyl) was incubated with [^{14}C]inositol 1-phosphate in the presence of the cell wall fraction of *M. smegmatis*, a significant amount of radioactivity was incorporated into chloroform-soluble materials. Two spots were detected by TLC of the chloroform-soluble products (Rf = 0.25 and 0.44, Fig. 1A, lane 3). The slower spot comigrated with standard PIP (dioleoyl) (Rf = 0.25) prepared as described earlier (Fig. 1A, lane 2). The other radioactive spot comigrated with standard PI (Rf = 0.44). The FAB-MS of the putative PIP gave signals of m/z 941 $(M\text{-}H)^-$ and 699 (phosphatidic acid) (Fig. 1C), which were consistent with the molecular weight and structure of dioleoylglycerophosphoinositol phosphate [PI(dioleoyl) + HPO_3 (PIP(dioleoyl))]. The faster moving spot had a signal of m/z 861 $(M\text{-}H)^-$ (Supplementary Fig. S1) on FAB-MS, identical to PI(dioleoyl). Thus, the two products were chromatographically and spectrometrically identified as PIP and PI, respectively.

The time course of synthesis of PIP and PI from CDP-DAG and [^{14}C]inositol 1-phosphate is shown in Fig. 1B. The incorporation of the radiolabel into PIP preceded that into PI. The apparent specific activity of this enzyme was 5.3 ± 0.83 nmol/h mg/protein (n = 4), ~2000 times higher than the specific activity of free [^{3}H]inositol incorporation into PI (2.5 pmol/h/mg) by *Mycobacterium* crude cell walls reported by Jackson *et al.* (*14*).

Cellular localization of PIP synthase activity was examined. Only the cell wall fraction had appreciable total and specific PIP synthase activity (Table I). The activity was almost completely dependent on the

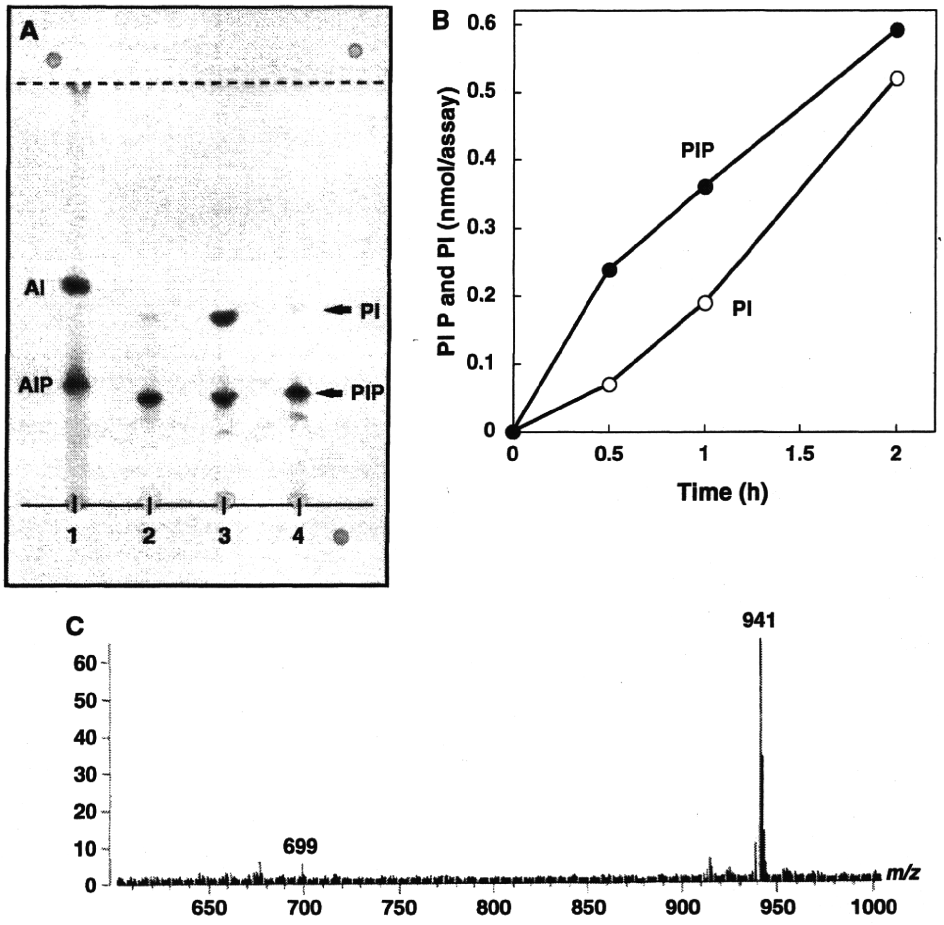

Fig. 1 Identification of the reaction products of PIP synthase. (A) Thin-layer chromatogram of ^{14}C-labelled products of the PIP (AIP)-synthase reaction. The source of the AIP synthase was cell homogenates of *E. coli* pET21a-MTH1691 (lanes 1 and 2), the purified cell wall fraction of *M. smegmatis* cell homogenates (lane 3) or cell homogenates of *E.coli* pET21a-abs-PIPS (CAM62975.1, PIP synthase of *M. abscessus*; lane 4). Lipid substrate in the enzyme reaction was CDP-archaeol (lane 1) or CDP-DAG (dioleoyl) (lanes 2–4). The products were extracted and developed by TLC. Radioactive spots were detected by autoradiography. s.f., solvent front; AI, archaetidylinositol; AIP, archaetidylinositol phosphate; PI, phosphatidylinositol; PIP, phosphatidylinositol phosphate. (B) Time-course of PIP synthase reaction. PIP and PI were formed from [^{14}C]inositol 1-phosphate and CDP-DAG (dioleoyl) catalysed by the purified cell wall fraction of *M. smegmatis* cell homogenates. The reaction was stopped at the indicated time points by the addition of 0.1 M HCl/methanol, radioactivity of chloroform-soluble products was counted. The ratio of PIP and PI was determined by autoradiography after TLC development of the chloroform-soluble products. (C) Negative ion FAB-mass spectra of PIP enzymatically synthesized from CDP-DAG (dioleoyl) and *myo*-inositol 1-phosphate (non-radiolabelled).

Table I. Incorporation of [^{14}C]inositol 1-phosphate (PIP synthase activity) and free [^{3}H]inositol into lipids (PIP and PI) using *M. smegmatis* cell wall, membrane and cytosol fractions or crude cell walls.

	PIP synthase activity					
	[^{14}C]Inositol 1-phosphate			[^{3}H]Inositol		
Fraction	Total activity (nmol/h)	Percent	Specific activity (nmol/h/mg)	Total activity (nmol/h)	Percent	Specific activity (nmol/h/mg)
Purified cell wall[a]	42	85	6.3	0.11	90	0.017
Membrane	4.4	9	0.6	0.0080	7	0.001
Cytosol	3.3	7	0.1	0.0049	4	0.000
Crude cell wall[b]	–	–	2.7	–	–	0.078

Assay was performed as described in 'Experimental Procedures' section with CDP-DAG(dioleoyl) and various enzyme preparations. [a]*Mycobacterium smegmatis* purified cell walls were obtained by centrifugation through a 60% Percoll layer. [b]*Mycobacterium smegmatis* crude cell walls were obtained from pellets upon centrifugation between 3000 r.p.m. for 10 min and 27,000*g* and resuspended in buffer.

presence of CDP-DAG and *myo*-inositol 1-phosphate (Table II). Differences in the fatty acyl group composition of CDP-DAG significantly affected PIP synthase activity (~50%).

To determine the reaction sequence of synthesis of PIP and PI, [^{14}C]PIP and [^{14}C]PI synthesized from the incubation of CDP-DAG (dipalmitoyl) and [^{14}C]inositol 1-phosphate for 4 h were isolated by

Table II. Requirements for PIP synthase.

[^{14}C]Inositol 1-phosphate	Source of enzyme	CDP-DAG	Relative incorporation, %
+[a]	*Mycobacterium smegmatis* purified cell walls	CDP-DAG (dioleoyl)	100
+	*Mycobacterium smegmatis* purified cell walls	CDP-DAG (dipalmitoyl)	54
+	*Mycobacterium smegmatis* purified cell walls	None	1
−[b]	*Mycobacterium smegmatis* purified cell walls	CDP-DAG (dioleoyl)	1
+	None	CDP-DAG (dioleoyl)	0
+	*Escherichia coli* pET21a-abs-PIPS[c]	CDP-DAG (dioleoyl)	292
+	*Escherichia coli* pET21a[d]	CDP-DAG (dioleoyl)	1

The reaction mixture of the PIP synthase reaction is described in 'Experimental Procedures' section. After incubation at 37°C for 1 h, radioactivity in the chloroform soluble materials was counted. [a][^{14}C]Inositol 1-phosphate was synthesized from [^{14}C]glucose 6-phosphate in a complete inositol phosphate synthase reaction mixture with the supernatant fraction of the *Methanothermobacter thermautotrophicus* homogenate. [b]The solution included only [^{14}C]glucose 6-phosphate as the radiolabelled material. [c]Homogenate of *E. coli* pET21a-abs-PIPS (CAM62975.1, PIP synthase of *Mycobacterium abscessus*). [d]Homogenate of *E. coli* pET21a.

TLC. The purified [^{14}C]PIP was converted to [^{14}C]PI in the presence of the cell wall fraction of *M. smegmatis* cell homogenates (Fig. 2, lane 2). Similar results were obtained in the case of [^{14}C]PIP (dioleoyl) without purification synthesized from CDP-DAG (dioleoyl) by the homogenate of *E. coli* carrying pET21a-mari-PIPS plasmid (Supplementary Fig. S2). The PIP phosphatase activity was localized in the cell wall fraction of *M. smegmatis* cells. On the other hand, [^{14}C]PIP was not formed from [^{14}C]PI in the presence of the cell wall fraction of *M. smegmatis* cell homogenates (Fig. 2, lane 4; Supplementary Fig. S2, lane 4).

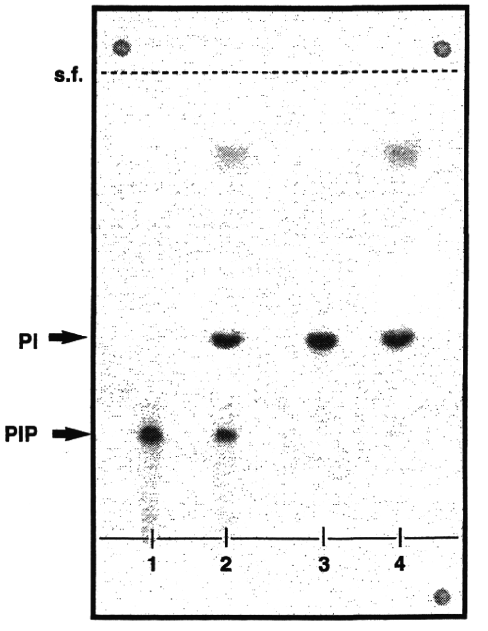

Fig. 2 Conversion of PIP to PI by the purified cell wall fraction of *M. smegmatis* cell homogenates (PIP phosphatase). [^{14}C]PIP and [^{14}C]PI were prepared from CDP-DAG (dipalmitoyl) and [^{14}C]inositol 1-phosphate using the PIP synthase reaction conditions described in the 'Experimental Procedures' section. The purified [^{14}C]PIP (lanes 1 and 2) or the purified [^{14}C]PI (lanes 3 and 4) was incubated at 37°C for 4 h with the cell wall fraction of *M. smegmatis* homogenate (lanes 2 and 4) or without the cell wall fraction (lanes 1 and 3). Other constituents in the reaction mixture were the same as in the PIP synthase reaction mixture without [^{14}C]inositol 1-phosphate. After the reaction, the lipids were extracted, separated by TLC, and recorded by autoradiography.

Cloning of a PIP synthase and characterization of the recombinant enzyme

The nucleic acid sequences of the cloned PIP synthase genes of *M. bovis* BCG, *M. smegmatis* mc^2 155 and *M. abscessus* were completely compatible with the sequences registered in the genome data base (http://gib.genes.nig.ac.jp/). The sequence of the cloned PIP synthase gene of *M. bovis* BCG was the same as that of *M. tuberculosis* (CAE55505.1) (Fig. 3). The sequence of the cloned PIP synthase gene of *M. marinum* was different from that of *M. marinum* M (ACC40540.1). The nucleic acid and amino acid sequence (AB559817) identities between the laboratory strain and *M. marinum* M (ACC40540.1) were 86% (614/710 bases) and 88% (207/234 amino acids), respectively. A typical sequence of a CDP-alcohol phosphatidyltransferase motif (*23*) was found in all of the amino acid sequences (Fig. 3). All of the *E. coli* cell homogenates in which the PIP synthase genes of four *Mycobacterium* species (*M. bovis* BCG, *M. marinum*, *M. smegmatis* mc^2 155 and *M. abscessus*) were expressed, had sufficient PIP synthase activity (9.0–15.5 nmol/h/mg). A main reaction product was PIP, based on TLC (Fig. 1A, lane 4). *Escherichia coli* pET21a cell homogenates carrying an empty vector possessed little PIP-synthesis activity (Table II). PI synthase activity (incorporation of free [^{3}H]inositol into lipid) was, however, not detected in the *E. coli* cell homogenates in which the PIP-synthase gene was expressed. Therefore, we concluded that the putative PIP-synthase genes are the structural genes that encode PIP synthase but not PI synthase, and PIP synthesis from CDP-DAG and *myo*-inositol 1-phosphate was catalysed by a single enzyme.

Inositol kinase activity

Although we demonstrated that PI was synthesized from CDP-DAG and inositol 1-phosphate via PIP, Salman *et al.* (*10*) reported the incorporation of free inositol into PI in the presence of mycobacterial cell walls. We attempted to confirm the reaction and to clarify the physiological significance of these reactions related to PI metabolism. Free [^{3}H]inositol was incorporated into lipids in the presence of *M. smegmatis* purified cell walls under the same conditions described

```
TUB     MSKLPFLSRAAFARITT-PIARGLLRVGLTPDVVTILGTTASVAGALTLF
BCG     MSKLPFLSRAAFARITT-PIARGLLRVGLTPDVVTILGTTASVAGALTLF
MAR     MSKAPFLSRAAFARVTN-PLARGLLRIGLTPDAVTIIGTTASVAGALVLF
SME     MSNVYLMTRAAYVKLSR-PVAKAALRAGLTPDIVTLAGTAAAVIGALTLF
ABS     MSG--LLSRETFAKITN-PLASALLRAGFTPDTVTIFGTAASVVAALTLF
MTH     MPDINESMLNQFRPVIRRFIDPIADRIALPADYITLTGFLVACAASAG-Y
PFU     ----MLSNLRPLAKKPLEKIAEPFSKLGITPNQLTMVGFFLSLLASYEYY
                          :     : .:..: :*: *   :   .:  :

TUB     PMGKLFAGACVVWFFVLFDMLDGAMARERGGGTRFGAVLDATCDRISDGA
BCG     PMGKLFAGACVVWFFVLFDMLDGAMARERGGGTRFGAVLDATCDRISDGA
MAR     PMGKLFPGACVVWFFVLFDMLDGAMARERGGGTRFGAVLDAACDRISDGA
SME     PIGQLWWGAVVVSFFVLADMLDGAMAREQGGGTRFGAVLDATCDRLGDGA
ABS     PTGHLFWGGMAVWLFAMFDMLDGAMARARGGGTRFGAVLDATCDRVADGA
MTH     ASGSLITGAALLAASGFIDVLDGAVARRRFRPTAFGGFLDSTLDRLSDGI
PFU     LNNQVFG-SLILLLGAFLDALDGSLARLTGRVTKFGGFLDSTMDRLSDAA
          . :   .  :    : * ***::**     * **..**:: **:.*.

TUB     VFCGLLWWIAFHMRDRPLVIATLICLVTSQVISYIKARAEASG-LRGDGG
BCG     VFCGLLWWIAFHMRDRPLVIATLICLVTSQVISYIKARAEASG-LRGDGG
MAR     VFGGLLWWVAFGMRDRLLVVATLICLVTSQVISYIKARAEASG-LRGDGG
SME     VFAGLTWWAAFGLDSPSLVVATLICLVTSQVISYIKARAEASG-LRGDGG
ABS     VFAGLVWWAAFGWGSTSLVVATLICMITSQVISYVKARAEASG-LRADGG
MTH     IIIGITAGGFTGLLTG------LLALHSGLMVSYVRARAESLG-IECAVG
PFU     IIFGIALGELVNWKVA------FLALIGSYMVSYTRCRAELAGSGTLAVG
        :: *:                  ::.:  . ::** :.***  *      *

TUB     FIERPERLIIVLTGAGVSDFPFVPWPPALSVGMWLLAVASVITCVQRLHT
BCG     FIERPERLIIVLTGAGVSDFPFVPWPPALSVGMWLLAVASVITCVQRLHT
MAR     IIERPERLIIVLAGAGVSDFPFIAWPPALPVAMWLLAVTSVITCGQRLYT
SME     IIERPERLVIVLIGAGLSDLPFFPLPWTLHVAMWVLAVASVVTLLQRVHA
ABS     LIERPERLIIVLAGAIFSGGFGVQWP--LHTAMWVLAVASLVTVAQRMHA
MTH     IAERAERIIIILAGSLAG---YLIHPWFMDAAIIVLAALGYFTMIQRMIY
PFU     IAERGERLLILVIAGLFG---------IIDIGVYLVAILSWITFLQRVYE
        : ** **::*:: ..  .          :  .: ::*  . .*  **:

TUB     VWTSPGAID----------------RMAIPGKGDR
BCG     VWTSPGAID----------------RMAIPGKGDR
MAR     VWTSPGATDLLVPSAPVRDDDAQGHPRSGDPGKTQR
SME     VRTSPGAMEPLHP------------ANGEKPETSEP
ABS     VRTSPGALDLLPNS----------DAGQDTAETNQP
MTH     VWQRLK------------------------------
PFU     AKKRLEK-----------------------------
```

Fig. 3 Multiple alignment of PIP Synthase and AIP Synthase. Genes homologous to *Methanothermobacter thermautotrophicus* (MTH1691) gene were identified in mycobacterial genome. The genes were tentatively annotated as PIP synthase. The amino acid sequence data of CAE55505.1, *Mycobacterium tuberculosis* (TUB); CAL72625.1, *M. bovis* (BCG); ACC40540.1, *M. marinum* (MAR); ABK73364.1, *M. smegmatis* (SME); CAM62975.1, *M. abscessus* (ABS); MTH1691, *Methanothermobacter thermautotrophicus* (MTH); PFU0462, *Pyrococcus furiosus* (PFU) were obtained from the NCBI site (www.ncbi.nih.gov). Multiple alignment of the seven sequences was constructed using the alignment software CLUSTAL W 1.83. Underlined sequences are CDP-alcohol phosphatidyltransferase motif.

by Salman *et al.* (*10*). The specific activity of [^{3}H]inositol incorporation, however, was only 0.27% that of [^{14}C]inositol 1-phosphate incorporation (Table I), as low as that reported by Salman *et al.* The products of free [^{3}H]inositol incorporation were identified by TLC as PI (the major spot) and PIP (the minor spot) (Fig. 4A, lane 1). The isolated minor spot (PIP) was converted to PI with *M. smegmatis* cell walls (Fig. 4B, lane 2), namely PIP was a precursor of PI. Although PIP formation requires both CDP-DAG and inositol 1-phosphate (Table II), inositol 1-phosphate was not added to this reaction. This suggests that inositol 1-phosphate is formed in the reaction mixture. Water-soluble inositol metabolites in the free [^{3}H]inositol incorporation reaction mixture were analysed by anion-exchange chromatography (Fig. 4C). Before the reaction started, all [^{3}H]inositol-derived materials were eluted with water and no ^{3}H material was retained on the column. After 2 h incubation, 5% of ^{3}H material was retained on the column by washing with water and eluted in the same fraction as inositol phosphate (0.1 M formic acid/0.2 M ammonium formate) (*22*) (Fig. 4C). This finding suggests that inositol was phosphorylated, probably by ATP in the *M. smegmatis* cell walls (possibly by inositol kinase).

PI/Inositol exchange reaction in Mycobacteria

As described earlier, in the presence of CDP-DAG and ATP, a small amount of [^{3}H]inositol was incorporated

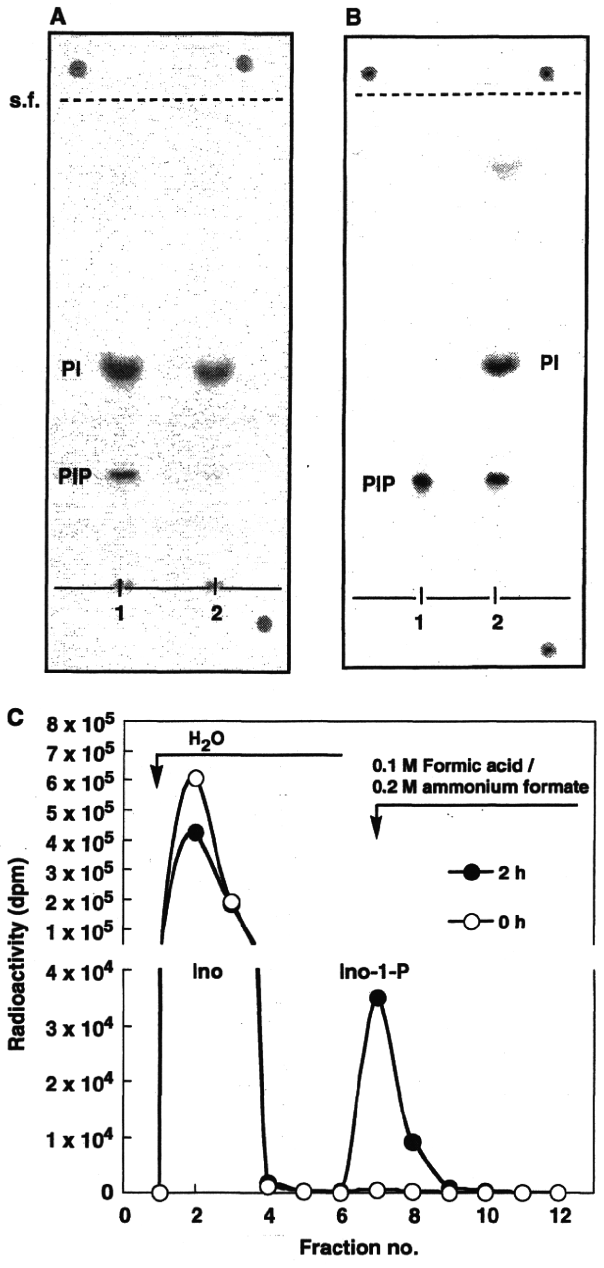

Fig. 4 Analysis of the reaction products from the free [^{3}H]inositol incorporation reaction by the purified *M. smegmatis* cell wall fraction. (A) Thin-layer chromatogram of ^{3}H-labelled $CHCl_3$-soluble products of the free [^{3}H]inositol incorporation reaction with CDP-DAG (dioleoyl) (lane 1) or without CDP-DAG (lane 2). (B) Conversion of [^{3}H]PIP to [^{3}H]PI. [^{3}H]PIP was prepared from [^{3}H]inositol and CDP-DAG (dipalmitoyl) as described in the 'Experimental Procedures' section. The purified [^{3}H]PIP was incubated at 37°C for 4 h with the cell wall fraction of *M. smegmatis* cell homogenate (lane 2) or without the cell wall fraction (lane 1). (C) Elution profiles of ^{3}H-labelled water-soluble products of free [^{3}H]inositol incorporation reaction by an anion-exchange column. The crude cell walls of *M. smegmatis* were incubated with free [^{3}H]inositol in the presence of 1 mM ATP without CDP-DAG for 0 or 2 h. The water-soluble components were applied to a Dowex-1 anion-exchange column and eluted with water and 0.1 M formic acid/0.2 M ammonium formate. Fractions (2 ml) were collected and radioactivity was measured. Authentic inositol phosphate was detected by phosphate determination.

into PI and PIP in the presence of *M. smegmatis* cell walls (Fig. 4A, lane 1). It should be noted that in the absence of CDP-DAG only the PI spot was detected (Fig. 4A, lane 2). The amount of [^{3}H]inositol incorporated into PI was 91% that obtained in the reaction with CDP-DAG (Table III). That is, the addition of CDP-DAG had almost no effect on inositol incorporation into PI. A reaction that proceeds without the addition of CDP-DAG is generally assumed to be a PI/inositol exchange reaction (*24*). Although PI as an acceptor of inositol was not added to the reaction mixture in this case, the cell wall fraction contains sufficient amounts of PI for the exchange reaction (*2*, *10*). Thus, the incorporation reaction of free [^{3}H]inositol into PI without CDP-DAG was concluded to be a PI/inositol exchange reaction.

The addition of PI (40 nmol) had no effect on free [^{3}H]inositol incorporation by the homogenate of *E. coli* pET21a-abs-PIPS. We also concluded that PIP synthase did not carry PI/inositol-exchange activity.

Discussion

These findings clearly demonstrated that mycobacterial PI was synthesized from CDP-DAG and 1L-*myo*-inositol 1-phosphate via PIP, which was dephosphorylated to PI. The time course of [^{14}C]inositol 1-phosphate incorporation into PIP and PI by the purified cell walls also supported this reaction sequence. PIP was not formed from PI by phosphorylation. Two possible enzyme activities, PIP synthase and PIP phosphatase, were detected in the cell wall fraction of *M. smegmatis*. The apparent specific activity of PIP synthesis of the mycobacterial cell wall fraction was comparable to yeast PI synthase activity in the membrane fraction. Consequently, we concluded that the main PI synthesis pathway in mycobacteria proceeded as the following new reaction sequence (Equations 6 and 7; see also Fig. 5).

$$\text{CDP-DAG} + \text{inositol 1-phosphate} \rightarrow \text{PIP} + \text{CMP} \quad (6)$$

$$\text{PIP} \rightarrow \text{PI} + \text{Pi} \quad (7)$$

The stereostructure of the phosphoinositol moiety of mycobacterial PI (*25*) is identical to that of soy bean (*26*) and *M. thermautotrophicus* (1D-*myo*-inositol 1-phosphate) (*27*); therefore, its precursor must be 1L-*myo*-inositol 1-phosphate. Bachhawat and Mande (*28*) identified an inositol 1-phosphate synthase homologue (*INO1*) in *M. tuberculosis* that functionally complements an *INO1*-deletion mutation in *S. cerevisiae*. This finding suggested that the reaction product of mycobacterial inositol 1-phosphate synthase is likely 1L-*myo*-inositol 1-phosphate. On the other hand, the complete structure of the reaction product of inositol 1-phosphate synthase of *M. thermautotrophicus* was determined to be 1L-*myo*-inositol 1-phosphate (*16*). Therefore, methanoarchaeal [^{14}C]inositol 1-phosphate was used as the substrate for the mycobacterial

PIP-synthase reaction. Because significant activity was detected, 1L-*myo*-inositol 1-phosphate is an adequate substrate for mycobacterial PIP synthase.

We reexamined Salman *et al.*'s experiments (*10*) of the PI synthesis reaction in mycobacterial cells from CDP-DAG with free inositol in the presence of ATP and glucose. In our experiments, [^{3}H]inositol was also incorporated into lipids in the presence of the *M. smegmatis* cell wall fraction under the same conditions. The specific activity of [^{3}H]inositol incorporation, however, was quite low (0.27%) compared with [^{14}C]inositol 1-phosphate incorporation (Table I). In contrast to mycobacterial cell walls, the recombinant PIP synthase-containing *E. coli* cell homogenates did not have any PI synthase activity. If PI was synthesized from CDP-DAG and inositol by a PI synthase reaction, another enzyme besides PIP synthase must exist in the mycobacterial cell walls.

Table III. Effect of components in the reaction mixture on incorporation of free [^{3}H]inositol into lipid by the purified cell walls of *M. smegmatis*.

Reaction mixture	Relative incorporation (%)
Complete	100
−CDP-DAG	91
−ATP	84
−CDP-DAG, −ATP	72
−Glucose	126

The complete reaction mixture contained 2.5 μM [^{3}H]inositol (0.5 nmol, 74 kBq/Assay), 40 nmol CDP-DAG (dioleoyl), 0.1 mM ATP, 50 mM MOPS buffer (pH 7.9), 5 μM 2-mercaptoethanol, 10 mM $MgCl_2$, 5 mM glucose and *M. smegmatis* cell walls. After incubation at 37°C for 1 h, radioactivity in the chloroform soluble materials was counted.

In summary, we propose four possible reactions/pathways concerning inositol phospholipid metabolism:

(i) *De novo* synthesis from CDP-DAG and free inositol (Eucarya);
(ii) *De novo* synthesis from CDP-DAG (CDP-archaeol) and inositol 1-phosphate (Bacteria/Archaea);
(iii) PI/inositol exchange reaction (Eucarya); and
(iv) Phosphorylation of inositol by inositol kinase followed by the above reaction (ii).

Pathway (i) is well-established in eukaryotes. Pathway (ii) was just recently reported (*16*). Here, we discuss pathways (iii) and (iv) in greater detail. There are two results that support pathway (iv). First, during incubation for the free inositol incorporation reaction, inositol was anionically modified (probably phosphorylated because of the presence of ATP as a phosphoryl group donor; Fig. 4C). Second, [^{3}H]PIP was synthesized by an [^{3}H]inositol incorporation reaction with CDP-DAG and was converted to [^{3}H]PI by *M. smegmatis* cell walls (Fig. 4B, lane 2). These two results suggest that free inositol was phosphorylated to inositol 1-phosphate, which then reacted with CDP-DAG to form PIP.

Activity of the PI/inositol exchange reaction (iii) is usually measured in the absence of CDP-DAG (*24*, *29*). Even if CDP-DAG was omitted from the reaction mixture, but a significant, although small amount of free [^{3}H]inositol was incorporated into the lipid (Table III). Salman *et al.* (*10*) obtained a similar

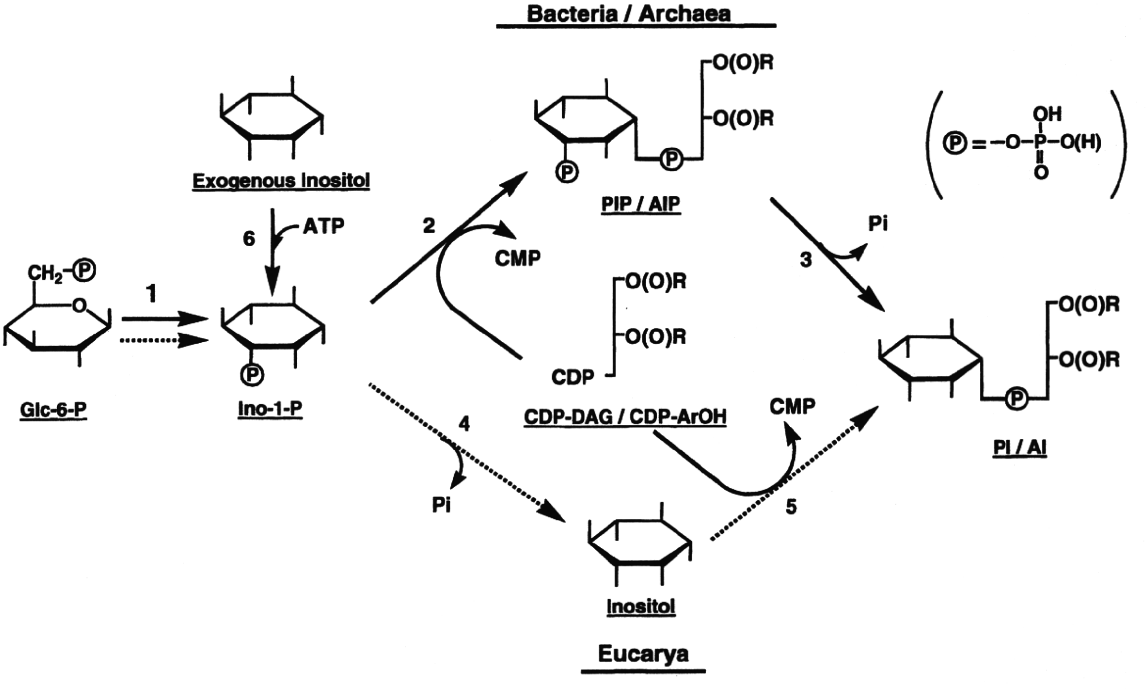

Fig. 5 Proposed biosynthetic pathway of PI and Archaetidyl-*myo*-inositol (AI) in Bacteria and Archaea (solid arrow), and Eucarya (broken arrow). Lane 1: 1L-*myo*-Inositol 1-phosphate synthase; lane 2: Phosphatidyl-*myo*-inositol phosphate (PIP) synthase/Archaetidyl-*myo*-inositol phosphate (AIP) synthase; lane 3: PIP phosphatase/AIP phosphatase; lane 4: 1L-*myo*-Inositol 1-phosphate phosphatase; lane 5: Phosphatidyl-*myo*-inositol (PI) synthase; lane 6: Inositol kinase.

result and explained that endogenous CDP-DAG reacted with the free inositol. However, the cell walls are considered to contain very little CDP-DAG because the cell walls have hardly any PIP synthase activity when exogenous CDP-DAG is not added to the reaction mixture (Table II). Furthermore, CDP-DAG added to the reaction mixture did not stimulate free [^{3}H]inositol incorporation into lipid in the presence of *M. smegmatis* cell walls (Table III). These results exclude the possibility that free inositol directly reacted with CDP-DAG [i.e. pathway (i)]. Therefore, the incorporation reaction of free [^{3}H]inositol into PI without CDP-DAG was concluded to be a PI /inositol exchange reaction [i.e. pathway (iii)]. For the PI/inositol exchange reaction, an acceptor PI must be present in the reaction mixture. Although no exogenous PI was added to the reaction mixture, the cells walls, which contain sufficient PI for an exchange reaction, are a possible source of acceptor PI (*2, 10*).

It has been reported that PI synthesis and exchange of the inositol head are catalysed by a single PI synthase from yeast (*24*) and *Arabidopsis* (*30*), and that the PI/inositol exchange reaction is not the result of a traditional D-type phospholipase in soybean microsomes (*29*). The mechanism in eukaryotes, however, is not likely applicable to mycobacteria, because mycobacteria do not possess PI synthase and the exchange reaction is not due to PIP synthase. Therefore, we speculate that the PI/inositol exchange reaction in mycobacteria is exceptionally catalysed by phospolipase D. The PI/inositol exchange reaction seems to be an unusual form of phospholipid metabolism that does not necessarily lead to a net synthesis of PI. At this point, the physiologic significance of the exchange reaction is unknown.

The level of free [^{3}H]inositol incorporation into lipid in the reaction was almost the same with or without CDP-DAG (Table III). The major product of the [^{3}H]inositol incorporation reaction with CDP-DAG was PI (Fig. 4A, lane 1). These results support the notion that free [^{3}H]inositol incorporation was due to the PI/inositol exchange reaction (iii), but see below. PIP was also detected as a minor product of the [^{3}H]inositol incorporation reaction with CDP-DAG, but not without CDP-DAG (Fig. 4A). These results indicate that the phosphorylated inositol reacted with the exogenous CDP-DAG.

Salman *et al. (10)* synthesized the fluorescent analogue of CDP-DAG, CDP-C_6-NBD-DAG, When this fluorescent substrate was incubated with the *M. smegmatis* cell wall fraction, NBD-PI was synthesized (*10*). This result does not support the PI/inositol exchange pathway (iii), but rather suggests that reaction (ii) occurred after the inositol phosphorylation reaction (iv).

In conclusion, in *Mycobacterium* species PI is synthesized from CDP-DAG and inositol 1-phosphate via PIP (Fig. 5, reactions 2 and 3). This is the main *de novo* biosynthetic pathway of mycobacterial PI. In addition to the main pathway, a side entrance of free inositol into the main pathway by phosphorylation, which might be an inositol salvage pathway (Fig. 5, reactions 6, 2 and 3), and a PI/inositol exchange reaction occurred in the cell wall fraction of *M. smegmatis*.

Fortunately, we detected PIP as an intermediate of PI synthesis using an acidified solvent system, which is essential for extracting PIP because PIP is partitioned in the aqueous fraction and/or fluff with a neutral solvent due to its high polarity. This property was applied to isolate PIP from the other polar lipids, including PI.

During the course of this study, Morita *et al.* (*31*) independently detected PIP in *M. smegmatis* cells *in vivo*. Although they considered that PIP was formed from PI by phosphorylation, their data, such as the stimulation of PIP accumulation by the addition of a phosphatase inhibitor or the increase in PIP formation by the addition of CTP, suggests that PI is formed from PIP. Thus, the presence of PIP as a precursor of PI was confirmed *in vivo* and *in vitro* by an independent research group.

Because the PI synthetic mechanism involving PIP synthase in *Mycobacterium* species is clearly different from the mechanism of human and animal PI synthesis and PIP synthase and PI synthase discriminate substrates, PIP synthase is a promising target for the development of new anti-mycobacterium drugs, which might have an important impact given the recent emergence of multi-drug resistant strains of *M. tuberculosis*.

Supplementary Data

Supplementary Data are available at *JB* Online.

Funding

Japan Society for the Promotion of Science (JSPS), KAKENHI (22590409).

Conflict of interest

Patent pending (Japan Patent application No. 2009-272247) for the author Hiroyuki Morii.

References

1. Cegielski, J.P. (2010) Extensively drug-resistant tuberculosis: "There must be some kind of way out of here". *Clin. Infect. Dis.* **50**, S195–S200
2. Brennan, P.J. and Nikaido, H. (1995) The envelope of mycobacteria. *Annu. Rev. Biochem.* **64**, 29–63
3. Apostolou, I., Takahama, Y., Belmant, C., Kawano, T., Huerre, M., Marchal, G., Cui, J., Taniguchi, M., Nakauchi, H., Fournie, J.J., Kourilsky, P., and Gachelin, G. (1999) Murine natural killer cells contribute to the granulomatous reaction caused by mycobacterial cell walls. *Proc. Natl Acad. Sci. USA* **96**, 5141–5146
4. Brennan, P.J. and Crick, D.C. (2007) The cell-wall core of *Mycobacterium tuberculosis* in the context of drug discovery. *Curr. Top. Med. Chem.* **7**, 475–488
5. Chatterjee, D. and Khoo, K.H. (1998) Mycobacterial lipoarabimomannan: an extraordinary lipoheteroglycan with profound physiological effects. *Glycobiology* **8**, 113–120
6. Fratti, R.A., Chua, J., Vergne, I., and Deretic, V. (2003) *Mycobacterium tuberculosis* glycosylated phosphatidylinositol causes phagosome maturation arrest. *Proc. Natl Acad. Sci. USA* **100**, 5437–5442

7. Geijtenbeek, T.B.H., van Herrera-Velit, P., Koppel, E.A., Hernandez, M.S., Grauls, C.M.J.E.V., Appelmelk, B., and van Kooyk, Y. (2003) Mycobacteria target DC-SIGN to suppress dendritic cell function. *J. Exp. Med.* **197**, 7–17
8. Knutson, K.L., Hmama, Z., Herrera-Velit, P., Rochford, R., and Reiner, N.E. (1998) Lipoarabinomannan of *Mycobacterium tuberculosis* promotes protein tyrosine dephosphorylation and inhibition of mitogenactivated protein kinase in human mononuclear phagocytes. *J. Biol. Chem.* **273**, 645–652
9. Nigou, J., Zelle-Rieser, C., Gilleron, M., Thurnher, M., and Puzo, G. (2001) Mannosylated lipoarabinomannans inhibit IL-12 production by human dendritic cells: evidence for a negative signal delivered through the mannose receptor. *J. Immunol.* **166**, 7477–7485
10. Salman, M., Lonsdale, J.T., Besra, G.S., and Brennan, P.J. (1999) Phosphatidylinositol synthesis in mycobacteria. *Biochim. Biophys. Acta* **1436**, 437–450
11. Steiner, M.R. and Lester, R.L. (1972) *In vitro* studies of phospholipid biosynthesis in *Saccharomyces cerevisiae*. *Biochim. Biophys. Acta* **260**, 222–243
12. Chen, I.W. and Charalampos, F.C. (1965) Inositol 1-phosphate as intermediate in the conversion of glucose 6-phosphate to inositol. *Biochem. Biophys. Res. Commun.* **19**, 144–149
13. Eisenberg, J.F. (1967) D-*myo*-inositol 1-phosphate as product of cyclization of glucose 6-phosphate and substrate for a specific phosphatase in rat testis. *J. Biol. Chem.* **242**, 1375–1382
14. Jackson, M., Crick, D.C., and Brennan, P.J. (2000) Phosphatidylinositolis an essential phospholipid of mycobacteria. *J. Biol. Chem.* **275**, 30092–30099
15. Fischl, A.S., Homann, M.J., Poole, M.A., and Carman, G.M. (1986) Phosphatidylinositol synthase from *Saccahromyces cerevisiae*. *J. Biol. Chem.* **261**, 3178–3183
16. Morii, H., Kiyonari, S., Ishino, Y., and Koga, Y. (2009) A novel biosynthetic pathway of archaetidyl-*myo*-archaetidyl-*myo*-inositol phosphate from CDP-archaeol and D-glucose 6-phosphate in methanoarchaeon *Methanothermobacter thermautotrophicus* cells. *J. Biol. Chem.* **284**, 30766–30774
17. Morii, H., Nishihara, M., and Koga, Y. (2000) CTP: 2,3-di-*O*-geranylgeranyl-*sn*-glycero-1-phosphate cytidyltransferase in the methanogenic archaeon *Methanothermobacter thermoautotrophicus*. *J. Biol. Chem.* **275**, 36568–36574
18. Wheeler, P.R., Besra, G.S., Minnikin, D.E., and Ratledge, C. (1993) Stimulation of mycolic acid biosynthesis by incorporation of *cis*-tetracos-5-enoic acid in a cell-wall preparation from *Mycobacterium smegmatis*. *Biochim. Biophys. Acta* **1167**, 182–188
19. Bligh, E.G. and Dyer, W.J. (1959) A rapid method of total lipid extraction and purification. *Can. J. Biochem. Physiol.* **37**, 911–917
20. Bartlett, G.R. (1959) Phosphorus assay in column chromatography. *J. Biol. Chem.* **234**, 466–468
21. Smith, P.K., Krohn, R.I., Hermanson, G.T., Mallia, A.K., Gartner, F.H., Provenzaro, M.D., Fujimoto, E.K., Goeke, N.M., Olson, B.J., and Klenk, D.C. (1985) Measurement of protein using bicinchoninic acid. *Anal. Biochem.* **150**, 76–85
22. Berridge, M.J., Dawson, R.M.C., Downes, C.P., Heslop, J.P., and Irvine, R.F. (1983) Changes in the levels of inositol phosphates after agonist-dependent hydrolysis of membrane phosphoinositides. *Biochem. J.* **212**, 473–482
23. Williams, J.G. and McMaster, C.R. (1998) Scanning alanine mutagenesis of the CDP-alcohol phosphotransferase motif of *Saccharomyces cerevisiae* cholinephosphotransferase. *J. Biol. Chem.* **273**, 13482–13487
24. Klezovitch, O., Brandenburger, Y., Geindre, M., and Deshusses, J. (1993) Characterization of reaction catalyzed by yeast phosphatidylinositol synthase. *FEBS Lett.* **320**, 256–260
25. Ballou, C.E., Vilkas, E., and Lederer, E. (1963) Structural studies on the *myo*-inositol phospholipids of *Mycobacterium tuberculosis* (var. *bovis*, strain BCG). *J. Biol. Chem.* **238**, 69–76
26. Ballou, C.E. and Pizer, L.I. (1959) Synthesis of an optically active *myo*-inositol 1-phosphate. *J. Am. Chem. Soc.* **81**, 4745
27. Nishihara, M., Morii, H., and Koga, Y. (1989) Heptads of polar ether lipids of an archaebacterium, *Methanobacterium thermoautotrophicum*: structure and biosynthetic relationship. *Biochemistry* **28**, 95–102
28. Bachhawat, N. and Mande, S.C. (1999) Identification of the INO1 gene of *Mycobacterium tuberculosis* H37Rv reveals a novel class of inositol-1-phosphate synthase enzyme. *J. Mol. Biol.* **291**, 531–536
29. Sandelius, A.S. and Morre, D. J. (1987) Characteristic of a phosphatidylinositol exchange activity of soybean microsomes. *Plant Physiol.* **84**, 1022–1027
30. Justin, A.M., Kader, J.C., and Collin, S. (2002) Phosphatidylinositol synthesis and exchange of the inositol head are catalyzed by the single phosphatidylinositol synthase 1 from *Arabidopsis*. *Eur. J. Biochem.* **269**, 2347–2352
31. Morita, Y.S., Botte, Y.Y., Miyanagi, K., Callaghan, J.M., Patterson, J.H., Crellin, P.K., Coppel, R.L., Jacobe, H.B., Kinoshita, T., and McConville, M.J. (2010) Stress-induced synthesis of phophatidylinositol 3-phosphate in mycobacteria. *J. Biol. Chem.* **285**, 16643–16650

International Immunology, Vol. 22, No. 3, pp. 179–189
doi:10.1093/intimm/dxp126
Advance Access publication 5 February 2010

Transient role of $CD4^+CD25^+$ regulatory T cells in mycobacterial infection in mice

Yuriko Ozeki[1,2], Isamu Sugawara[3], Tadashi Udagawa[3], Toshiaki Aoki[3], Mayuko Osada-Oka[1], Yoshitaka Tateishi[1], Hajime Hisaeda[4], Yuji Nishiuchi[5], Nobuyuki Harada[3], Kazuo Kobayashi[6] and Sohkichi Matsumoto[1]

[1]Department of Bacteriology, Osaka City University Graduate School of Medicine, 1-4-3 Abeno-ku, Osaka 545-8585, Japan
[2]Sonoda Women's University, 7-29-1 Minamitsukaguchi-cho, Amagasaki, Hyogo 661-8520, Japan
[3]Mycobacterial Reference Center, The Research Institute of Tuberculosis, 3-1-24 Matsuyama Kiyose-shi Tokyo, 204-8533, Japan
[4]Department of Microbiology and Immunology, Graduate School of Medical Sciences, Kyushu University, 3-1-1 Maidashi, Higashi-ku, Fukuoka 812-8582, Japan
[5]Peptide Institute Inc., Protein Research Foundation, Minoh-shi, Osaka 562-8686, Japan
[6]Department of Immunology, National Institute of Infectious Diseases, Toyama 1-23-1, Shinjuku-ku, Tokyo 162-8640, Japan

Correspondence to: S. Matsumoto and Y. Ozeki; E-mail. sohkichi@med.osaka-cu.ac.jp and yuriozeki@med.osaka-cu.ac.jp

Transmitting editor: S. Koyasu

Received 22 April 2009, *accepted* 22 December 2009

Abstract

$CD4^+CD25^+$ regulatory T (Treg) cells cause immune suppression by inhibiting T cell effector functions and play pivotal roles not only in self-tolerance but also in immune response to parasitic microbial pathogens. Mycobacteria are major parasitic bacterial pathogens, but the role of $CD4^+CD25^+$ Treg cells in mycobacterial infection is not yet defined. In this study we found that, at the early stage of infection, depletion of $CD25^+$ cells reduced both bacterial load and granuloma formation in mice infected with *Mycobacterium tuberculosis* strains, such as *M. tuberculosis* Erdman or *M. tuberculosis* Kurono. However, at a later stage of infection, bacterial burden and histopathology were similar regardless of depletion of $CD25^+$ cells. Severe combined immunodeficient (SCID) mice reconstituted with $CD4^+CD25^-$ T cells alone or a combination of $CD4^+CD25^+$ and $CD4^+CD25^-$ T cells showed similar bacterial loads and survival kinetics after infection with *M. tuberculosis* Erdman. Consistent with *in vivo* data, *in vitro* studies revealed that mycobacterial antigens, purified protein derivative of tuberculin (PPD), failed to induce the suppressive function of $CD4^+CD25^+$ Treg cells to $CD4^+CD25^-$ effector T cells, as demonstrated by the lack of response of $CD4^+CD25^+$ T cells to PPD, in mice chronically infected with *Mycobacterium bovis* bacillus Calmette–Guérin and *M. tuberculosis*. Our data show that $CD4^+CD25^+$ Treg cells have a transient effect at the early stage of mycobacterial infection but, contrary to the expectation, have little impact on the overall course of infection.

Keywords: bacterial, T cells, rodent, inflammation, lung

Introduction

Mycobacteria are intracellular bacterial pathogens, which persistently infect eukaryotes, including mammals, and cause diseases not only following primary infection but also by reactivation from latent state. Several species of mycobacteria, such as *Mycobacterium tuberculosis* and *Mycobacterium bovis*, are known to cause human tuberculosis. The World Health Organization estimates that *M. tuberculosis* infects one-third of the world's population and is responsible for 2 million deaths each year (1). While the infection remains latent in 95% of the infected cases of *M. tuberculosis*, 5–10% of those who initially controlled the infection later develop active disease at some stage during their lifetime. To suppress intracellular growth of mycobacteria, macrophage activation by IFN-gamma is critical in both mice (2, 3) and humans (2, 3).

The important role of the $CD4^+CD25^+$ regulatory T (Treg) cells in immune response has recently been recognized. This T cell subset maintains immunologic self-tolerance and suppresses the onset of autoimmune diseases (4). The vast majority of Treg cells constitutively express CD25/IL-2 receptor alpha chain in the physiological state (5, 6). $CD4^+CD25^+$ Treg cells also express cytotoxic T-lymphocyte-associated protein 4 (CTLA-4; 7, 8), glucocorticoid-induced tumor necrosis factor receptor (GITR; 9, 10) and the transcription factor,

FoxP3 (11, 12). Some subsets of $CD4^+CD25^+$ Treg cells also produce effector cytokines, such as IL-10 and transforming growth factor (TGF)-β (13, 14). The defining feature of $CD4^+CD25^+$ Treg cells is their ability to inhibit the proliferation of T cells and IFN-gamma production through cell–cell contact (15, 16), possibly mediated by CTLA-4, and/or through the production of immunosuppressive cytokines, such as TGF-β and IL-10 (13, 14).

Recently, it has been reported that $CD4^+CD25^+$ Treg cells are also involved in suppressive immune responses during several infectious diseases. Depletion of $CD4^+CD25^+$ Treg cells enhances anti-microbial activity against diverse pathogens including the protozoan *Leishmania major* and *Plasmodium yoelii*, viruses such as HIV and Herpes simplex virus and bacteria such as *Helicobacter pylori* (17–21).

In spite of suggested importance of $CD4^+CD25^+$ Treg cells in parasitic pathogens, the knowledge in mycobacterial infection remains controversial (22–25). Kursar *et al.* and Scott-Browne *et al.* showed that Treg cells prevented protective immunity against *M. tuberculosis* infection by utilizing reconstituted and chimeric mice, respectively (22, 25). In contrast, Quinn *et al.* suggested minor role of $CD4^+CD25^+$ in both *Mycobacterium bovis* bacillus Calmette Guérin (BCG)-induced protection and natural mycobacterial infection (23, 24). In order to elucidate the roles of $CD4^+CD25^+$ Treg cells in mycobacterial infection more precisely, we carried out the experiments using Treg-deleted mice by antibody to CD25 molecule and SCID mice reconstituted with T cell subsets. We found that mycobacterial antigen-specific $CD4^+CD25^+$ Treg cells were hardly developed after mycobacterial infection in mice and therefore the function of $CD4^+CD25^+$ Treg cells was limited after the infection was established. Thus, $CD4^+CD25^+$ Treg cells have little impact on the overall course of mycobacterial infection.

Methods

Mice

Specific pathogen-free, female DBA/2 mice aged 6 weeks were purchased from Japan SLC (Shizuoka, Japan). BALB/c and SCID/BALB/c mice were purchased from Japan CLEA (Tokyo, Japan). All mice were maintained under specific pathogen-free conditions in the animal facilities of Osaka City University Graduate School of Medicine and in a biosafety-level-3 facility at The Research Institute of Tuberculosis according to the standard guidelines for animal experiments at each institute with approval of their ethical committees.

Depletion of $CD4^+CD25^+$ cells

A hybridoma cell line expressing anti-mouse CD25 monoclonal IgM [a monoclonal antibody against mouse CD25 (7D4), American Type Culture Collection, Manassas, VA, USA] was expanded as ascites in pristine-primed SCID mice (Wako, Osaka, Japan). The Ig-rich fraction was obtained by 30% ammonium sulfate precipitation of ascitic fluid followed by dialysis in PBS. An isotype-matched control IgM was purchased from eBioscience (San Diego, CA, USA). The protein concentration was determined by Bradford's method using BSA (Sigma–Aldrich, St Louis, MO, USA) as a standard. For depletion of $CD25^+$ cells in early stage of infection, mice were injected with 1 mg of 7D4 or control IgM intraperitoneally (i.p.) 1 day before, and then 3 and 10 days after *M. tuberculosis* infection. For depletion of $CD25^+$ cells in late stage of infection, mice were injected (i.p.) with 1 mg of 7D4 or control IgM at 60, 65 and 70 days after *M. tuberculosis* infection. Depletion of $CD4^+CD25^+$ cells was assessed by flow cytometry using a FACScan (Becton Dickinson, Franklin Lakes, NJ, USA). Peripheral blood leukocytes (PBLs) were obtained by incubation with 0.83% ammonium chloride solution at 37°C for 5 min to induce erythrocyte lysis. PBLs or splenocytes were stained with PE-conjugated anti-CD4 mAb (GK1.5, eBioscience) and FITC-conjugated anti-CD25 mAb (PC61, eBioscience). The data were analyzed by flow cytometry with using Cellquest™ software (Becton Dickinson).

Bacteria and infection

Mycobacterium bovis BCG Tokyo, *M. tuberculosis* H37Rv, *M. tuberculosis* Kurono (ATCC 35812) and *M. tuberculosis* Erdman were grown in 7H9 medium (Difco, Detroit, MI, USA) supplemented with 10% BSA, dextrose and catalase enrichment (Difco) and 0.05% Tween 80 at 37°C to mid-logarithmic phase, then stored in frozen aliquots as previously described (26). For infection with *M. tuberculosis* Kurono and *M. tuberculosis* Erdman, the nebulizer of a Middlebrook airborne infection apparatus (Glas-col, Terre Haute, IN, USA) was filled with 5 ml PBS containing 5×10^6 colony-forming units (CFU) of bacteria and the mice were airborne infected for 90 min by Glas-Col aerosol generator. This procedure deposits ~10 CFU of bacteria into the lungs. At 0, 3 and 5 weeks (and also 2 weeks in some experiments) post-infection, three to five mice per group were euthanized and the lungs, livers and spleens were harvested. The organs were homogenized in 1 ml sterile distilled water using a mortar and pestle and serial dilutions were plated onto Middlebrook 7H11 agar containing oleic acid, dextrose, albumin and catalase enrichment (Difco) (7H11-OADC agar). Bacterial numbers were counted using CFU after culturing at 37°C for 20–30 days. To investigate the role of $CD4^+CD25^+$ Treg cells in the late stage of infection, mice were airborne-infected with *M. tuberculosis* H37Rv as the same method described above and $CD25^+$ cells were depleted by 7D4 treatment on days 60, 65, and 70. At 75 days post-infection, eight mice per group were euthanized and bacterial numbers in lungs and spleens were determined by CFU count and histological evaluation were performed as the same procedures described above.

Isolation of $CD4^+CD25^+$ T cells and $CD4^+CD25^-$ T cells

BALB/c mice were infected i.p. with 5×10^4 CFU of *M. bovis* BCG Tokyo. $CD4^+CD25^+$ T cells and $CD4^+CD25^-$ T cells were purified from spleens of normal mice or chronically BCG-infected (>6 months post-infection) BALB/c mice using $CD4^+CD25^+$ regulatory T cell isolation kit (Miltenyl Biotec, Bergisch Gladgach, Germany) after depleting erythrocytes with 0.83% ammonium chloride solution. Obtained cells were labeled with PE-conjugated anti-CD25 mAb, stained with FITC-conjugated anti-CD4 mAb (eBioscience) and analyzed

by flow cytometer. The purity of selected populations was confirmed as >96%. Expression of foxp3 in the $CD4^+CD25^+$ T cell population was confirmed using flow cytometer after intracellular staining with anti-FITC-conjugated anti-mouse foxp3 mAb (eBioscience). $CD4^+CD25^+$ T cells stained by this procedure were >90% foxp3-positive. Non-$CD4^+$ cells of normal mice retained in the MACS separation column were flushed out and incubated for >2 h. Attached cells were used as antigen-presenting cells (APCs) after treatment with 20-Gy radiation. T cell populations and APCs were also isolated from DBA/2 mice chronically infected with *M. tuberculosis* as the similar procedure with BCG-infected mice described above. However, in this case, to obtain APCs, spleen cells of normal DBA/2 mice were incubated for >2 h and attached cells were treated with mitomycin C (50 μg zml^{-1}) for 30 min at 37°C instead of radiation.

In vitro T cell proliferation assay and measurement of cytokines

$CD4^+CD25^+$ T cells and $CD4^+CD25^-$ T cells were prepared to be 1×10^6 cells ml^{-1}. Various ratios of $CD4^+CD25^+$ T cells and $CD4^+CD25^-$ T cells were cultured for 5 or 7 days with 10 μg ml^{-1} of purified protein derivative of tuberculin (PPD) or anti-CD3 mAb (CEDARLANE, Canada) in the presence of 1×10^5 cells ml^{-1} of APC in 96-well plates in RPMI 1640 supplemented with 10% FCS, 2 mM L-glutamine, penicillin (100 U ml^{-1}), streptomycin (100 mg ml^{-1}) and 50 mM 2-mercaptoethanol. Proliferation was evaluated by pulsing cells with 1 μCi (37 kBq) per well [^{3}H]thymidine ([^{3}H]TdR) for 6 h and [^{3}H]TdR incorporation measured using a scintillation counter. In the experiments to analyze the function of T cells derived from *M. tuberculosis*-infected mice, proliferation was evaluated by incorporation of 5-bromo-2′-deoxyuridine (BrdU) using a commercially available kit (Cell proliferation ELISA, BrdU colorimetoric, Roche, Germany). Production of IFN-gamma, IL-10, IL-2 and IL-6 in the culture supernatant was measured using a commercially available ELISA kit (R&D System, Minneapolis, MN, USA).

Transfer of T cell population into SCID mice

$CD4^+CD25^+$ T cells and $CD4^+CD25^-$ T cells were purified from the spleens of BALB/c mice chronically infected with BCG using $CD4^+CD25^+$ Treg cell isolation kit. Totally, 7.5×10^5 $CD4^+CD25^-$ T cells or 7.5×10^5 $CD4^+CD25^+$ T cells either alone or in combination (7.5×10^5 $CD4^+CD25^-$ T cells and 7.5×10^4 $CD4^+CD25^+$ T cells) were transferred intravenously to cognate SCID mice (17). One day after transfer, recipient mice were infected aerogenically with *M. tuberculosis* Erdman as described above. Three weeks post-infection, five to eight mice were euthanized and bacterial burden was counted. The survival time course of seven mice per group was observed for up to 165 days post-infection.

Neutralization of IL-6 in culture supernatant

$CD4^+CD25^-$ T cells, $CD4^+CD25^+$ T cells and APCs were isolated from chronically BCG-infected mice according to the procedures described above. Anti-mouse IL-6-neutralizing mAb (Biolegend, San Diego, CA, USA) or isotype-matched control antibody (Southern Biotech, Birmingham, AL, USA) was added to the culture of $CD4^+CD25^-$ effector T cells either alone or in combination with $CD4^+CD25^+$ T cells at concentration of 0.02 μg ml^{-1} and cultured for 4 days in the presence of PPD or anti-CD3 mAb. IFN-gamma production and [^{3}H]TdR incorporation were measured after 4 days incubation.

Transfer of culture medium

T cell subsets were obtained from chronically BCG-infected mice as described above. $CD4^+CD25^-$ T cells/$CD4^+CD25^+$ T cells/APCs (1:0:0.1) or $CD4^+CD25^-$ T cells/$CD4^+CD25^+$ T cells/APCs (1:1:0.1) were cultured with PPD or anti-CD3 mAb for 7 days and each culture supernatant stored at −80°C until later use. Freshly isolated $CD4^+CD25^-$ T cells/$CD4^+CD25^+$ cells/APCs (1:0:0.1) or $CD4^+CD25^-$ T cells/$CD4^+CD25^+$ T cells/APCs (1:1:0.1) were cultured with stored supernatant:new medium (1:1) in the presence or absence of anti-CD3 mAb. On day 4, [^{3}H]TdR incorporation was measured as described above.

In vitro activation of $CD4^+CD25^+$ T cells

$CD4^+CD25^+$ T cells isolated from chronically infected BALB/c mice with BCG or *M. tuberculosis* H37Rv were incubated with Dynabeads Mouse CD3/CD28 T cell Expander (Invitrogen, Norway) at a bead:cell ratio of 2:1 adding 2000 U ml^{-1} of recombinant mouse IL-2 according to the manufacturer's protocol. Two days after incubation, the beads were

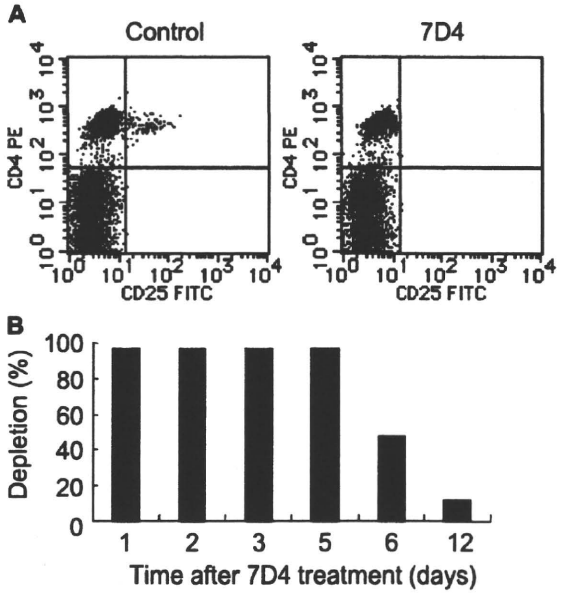

Fig. 1. Selective loss of $CD4^+CD25^+$ T cells by treatment with anti-CD25 mAb, 7D4. (A) Flow cytometric analysis of PBLs obtained from i.p.-injected mice with 1 mg of anti-CD25 mAb (7D4) or control IgM (control) 1 day after injection. Cells were stained with FITC-conjugated anti-CD25 mAb (PC61) and PE-conjugated anti-CD4 mAb (GK1.5). (B) Time course of the level of depletion of $CD4^+CD25^+$ T cell in PBL after a single dose of 7D4. Data are expressed as percent depleted relative to the $CD4^+CD25^+$ cell population in control IgM-treated mice. Data are mean of three mice per time point.

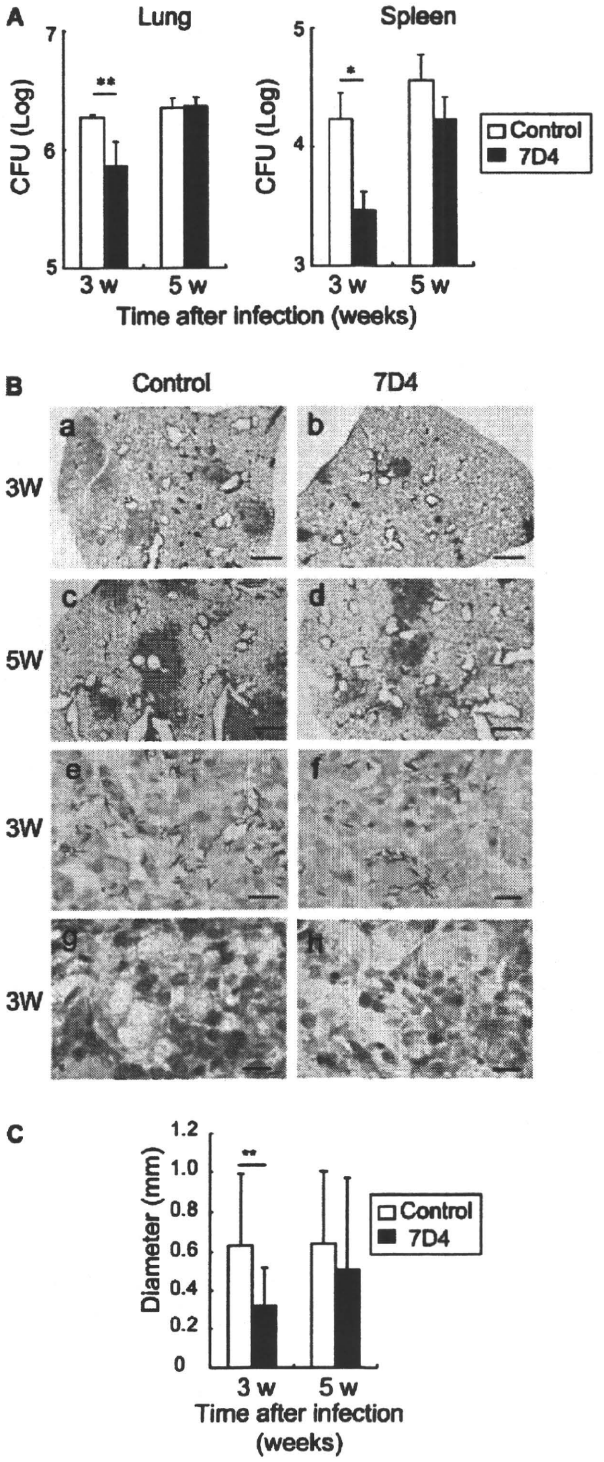

Fig. 2. The effect of $CD25^+$ cell depletion in *Mycobacterium tuberculosis* Kurono infection in mice. DBA/2 mice treated with 1 mg of 7D4, anti-CD25 mAb or control IgM were aerogenically infected with 5×10^6 CFU of *M. tuberculosis* Kurono. (A) Bacterial numbers were counted in lungs (left panel) and spleens (right panel) of mice treated with control IgM (open bars) or with 7D4, anti-CD25 mAb (closed bars). (B) Histopathological features of lungs from *M. tuberculosis* Kurono-infected mice. Lung sections were stained with H&E (a–d), Ziehl–Neelsen (e and f) and Giemsa (g and h). Granulomas mainly consisted of epithelioid macrophages (g and h). Numerous acid-fast bacteria were observed in granulomas of both control IgM-treated and anti-CD25 mAb-treated (7D4) mice. (a, c, e and g) Lungs sections from mice treated with control IgM. (b, d, f and h) Lungs sections from mice treated with 7D4. (a, b and e–h) Three weeks after infection. (c and d) Five weeks after infection. Bars, 500 μm (a–d), 10 μm (e-h). (C) The diameter of granulomatous lesions was measured in the lung sections from mice treated with control IgM (open bars) or with 7D4, anti-CD25 mAb (closed bars). Bars represent mean ±standard deviation of three to five mice. $^*P < 0.05$ versus control mice; $^{**}P < 0.01$ versus control mice.

removed from $CD4^+CD25^+$ T cells by magnet. After washing with medium, cells were used as activated $CD4^+CD25^+$ T cells. Freshly isolated $CD4^+CD25^-$ effector T cells were incubated with activated $CD4^+CD25^+$ T cells in the presence of PPD.

Histological analysis

Tissues were removed from mice at various intervals, fixed in 10% formalin and embedded in paraffin blocks. Sections (5 μm) were stained with hematoxylin and eosin (H&E), Ziehl–Neelsen or Giemsa methods. To evaluate the intensity of inflammatory response of the lung, the mean diameters of pulmonary granulomas were measured in three sections per mouse using Microanalyzer (Poladigital, Tokyo, Japan).

Statistical analysis

Results were analyzed by one-way analysis of variance (ANOVA) by SAS system R.8.1. Data were expressed as mean values ± standard deviation and considered significant if $P < 0.05$.

Results

Depletion of $CD25^+$ cells in early stage of infection causes transient effect on in vivo growth of M. tuberculosis Kurono and M. tuberculosis Erdman

7D4 is a mAb against mouse CD25. Administration of 1 mg 7D4 into a mouse resulted in the loss of >96% of $CD4^+CD25^+$ T cells in the peripheral blood and spleens (Fig. 1A). Loss of $CD25^+$ cells maintained at least for 5 days after 7D4 treatment (Fig. 1B). Depletion of $CD25^+$ cells by 7D4 protects mice from death caused by infection of *Plasmodium yoelii*, suggesting a role for $CD4^+CD25^+$ Treg cells in exacerbating malaria (21).

Using 7D4, we first depleted $CD25^+$ cells of DBA/2 mice and then infected animals with 5×10^6 CFU/mouse of *M. tuberculosis* Kurono, which was clinically isolated strain in Japan, by airborne infection. Bacterial load in lung and spleen, and histopathology of the lung were monitored at 3 and 5 weeks post-infection. *Mycobacterium tuberculosis* Kurono multiplied to approximately 2×10^6 CFU per lung 3 weeks post-challenge and maintained these bacterial numbers 5 weeks post-challenge. In spleens, we detected 2×10^4 and 3×10^4 CFU per organ 3 and 5 weeks

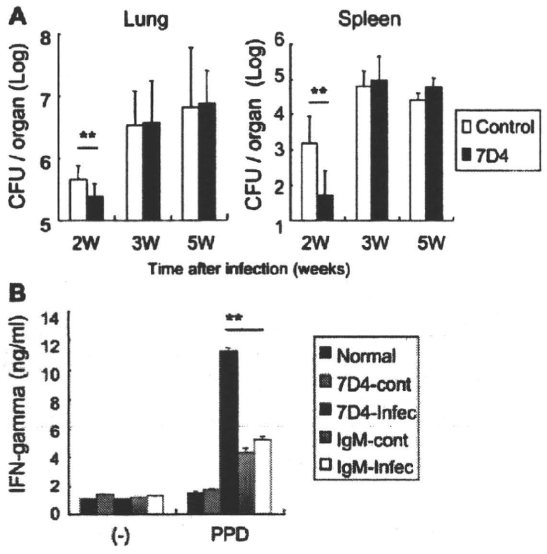

Fig. 3. The effect of CD25$^+$ cell depletion in *Mycobacterium tuberculosis* Erdman infection. (A) Control IgM-treated mice (open bars) and 7D4 anti-CD25 antibody-treated-mice (closed bars) were aerogenically infected with 5 × 10^6 CFU of *M. tuberculosis* Erdman. Bacterial numbers of lungs and spleens were measured at 2, 3 and 5 weeks post-infection. $^{**}P < 0.01$ versus control mice. (B) CD4$^+$ T cells from non-infected mice with 7D4 treatment (7D4-cont), *M. tuberculosis*-infected mice with 7D4 treatment (7D4-Infec), non-infected mice with control IgM treatment (IgM-cont) or *M. tuberculosis*-infected mice with control IgM treatment (IgM-Infec) were cultured with APC in the presence (PPD) or absence (−) of 10 μg ml^{-1} PPD for 7 days. Production of IFN-gamma in the culture supernatants was analyzed. $^{**}P < 0.01$: *Mycobacterium tuberculosis*-infected mice with control IgM treatment (IgM-Infec) versus *M. tuberculosis*-infected mice with 7D4 treatment (7D4-Infec).

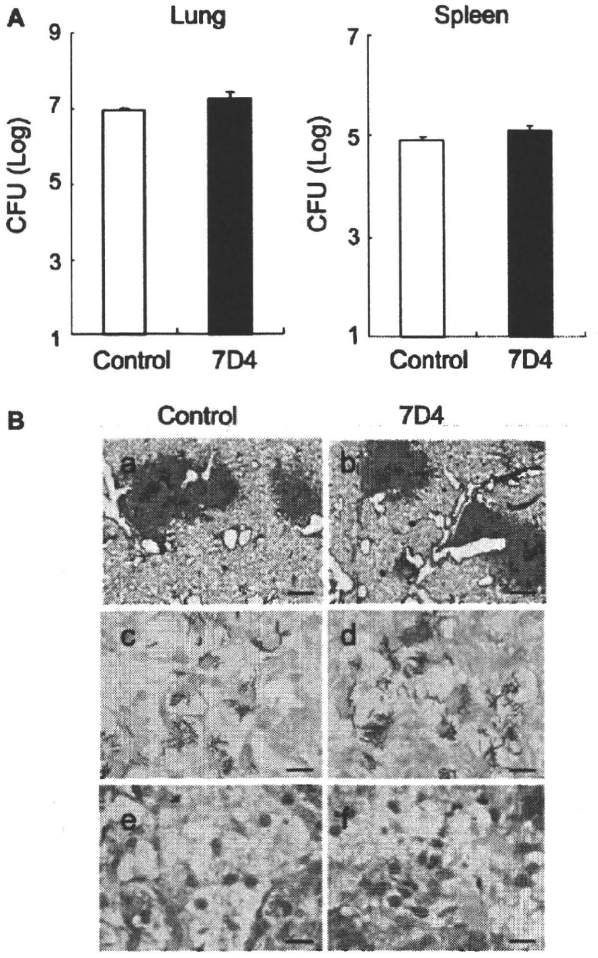

Fig. 4. The effect of depletion of CD25$^+$ cell in chronically infected mice with *M. tuberculosis*. DBA/2 mice were aerogenically infected with 5 × 10^6 CFU of *M. tuberculosis* H37Rv. Two months after infection, mice were treated with 1 mg of 7D4 or control IgM three times with 4 days interval. Five days later from final treatment, mice were sacrificed and analyzed. (A) Bacterial numbers in lungs (left panel) and spleens (right panel) of mice treated with control IgM (open bars) or 7D4 (closed bars). (B) Lung sections were stained with H&E (a and b), Ziehl–Neelsen (c and d) and Giemsa (e and f). Granulomas mainly consisted epithelioid macrophages (e and f). Numerous acid-fast bacteria were observed in granulomas of both control IgM- and 7D4-treated mice. (a, c and e) Lungs sections from mice treated with control IgM. (b, d and f) Lungs sections from mice treated with 7D4. Bars, 500 μm (a and b), 10 μm (c–f). Bars represent mean ±standard deviation of eight mice.

post-challenge, respectively (Fig. 2A). Depletion of CD25$^+$ cells resulted in significantly lower bacterial number in both lung and spleen 3 weeks after challenge; however, this effect became marginal 5 weeks post-challenge (Fig. 2A). Numerous bacteria were observed in granulomas of 7D4-treated and control mice after infection (Fig. 2B, e and f), consistent with higher bacterial burdens revealed by plating of organ homogenates (Fig. 2A). Histological examination of the lung correlated with the CFU results; 3 weeks post-infection, depletion of CD25$^+$ cells resulted in decreased granuloma formation compared with mice treated with control IgM, but normalized 5 weeks after challenge [Fig. 2B(a–d) and C]. Histopathology showed that granuloma cellular composition did not differ between 7D4-treated mice and control mice, which consisted predominately of epithelioid macrophages (Fig. 2B, g and h). Thus in *M. tuberculosis* Kurono infection, the effect of CD25$^+$ cell depletion was limited to the early phase of infection only.

To determine whether the transient effect of CD25$^+$ cells is specific for *M. tuberculosis* Kurono, we performed similar experiments employing another commonly used mycobacterial strain, *M. tuberculosis* Erdman. Similar results were observed in bacterial burdens: 7D4-treated mice revealed significantly lower bacterial numbers than those of IgM-treated mice at early stage (2 weeks post-infection), but not 3 weeks or 5 weeks post-challenge (Fig. 3A). Splenic CD4$^+$ T cells derived from 7D4-treated mice at this time point produced significantly higher levels of IFN-gamma than those of IgM-treated mice when stimulated with PPD (Fig. 3B).

We also examined the effects of depletion of CD25$^+$ cells on the survival of another mycobacterial strain, *Mycobacterium bovis* bacillus Calmette-Guérin (BCG). DBA/2 or BALB/c mice depleted of CD25$^+$ cells by 7D4 were challenged with BCG intravenously and the survival of BCG in the lungs

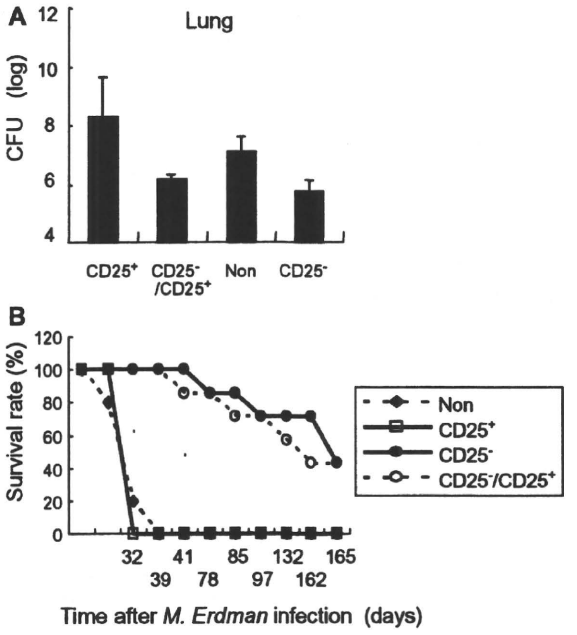

Fig. 5. Bacterial burden and survival kinetics of reconstituted SCID mice with T cell subsets after infection of *Mycobacterium tuberculosis* Erdman. (A) T cell subsets were isolated from spleens of chronically BCG-infected mice. SCID mice were reconstituted with 7.5×10^5 of $CD4^+CD25^+$ T cells only ($CD25^+$), 7.5×10^5 of $CD4^+CD25^-$ T cells and 7.5×10^4 of $CD4^+CD25^+$ T cells ($CD25^-/CD25^+$), untransferred (Non), and 7.5×10^5 of $CD4^+CD25^-$ T cells only ($CD25^-$). One day after reconstitution, naive or T cell subset-reconstituted SCID mice were aerogenically infected with 5×10^6 CFU *M. tuberculosis* Erdman. (B) Survival rates of naive or reconstituted SCID mice after infection. Time course of survival was examined up to 165 days post-infection. Five to eight mice per group were analyzed.

post-challenge was monitored. Unlike *M. tuberculosis*, there was no marked increase in BCG levels in the mouse lungs. Depletion of $CD25^+$ cells did not alter the survival ratio of BCG in the lungs of DBA/2 and BALB/c mice 3 and 5 weeks post-infection, although *in vitro* stimulation with PPD, lymphocytes derived from 7D4-treated mice at 3 weeks after challenge produced higher amount of IFN-gamma than those from control IgM-treated mice (data not shown).

Depletion of $CD25^+$ cells in the chronic stage of infection does not affect the bacterial burdens and pathology

We next examined the effects of depletion of $CD25^+$ cells in the late stage of mycobacterial infection. DBA/2 mice were airborne-infected with *M. tuberculosis* H37Rv and $CD25^+$ cells were depleted by 7D4 treatment after 60, 65 and 70 days later. Five days later from the final treatment of 7D4, we analyzed the bacterial burden and histology in the organs. Bacterial numbers of lungs and spleens in 7D4-treated mice were rather slightly higher than those in control IgM-treated mice; however, significant differences were not observed (Fig. 4A). Pulmonary granuloma formation was conspicuous in both 7D4-treated mice and control IgM-treated mice (Fig. 4B, a and b). Cellular composition of granuloma did not differ between 7D4-treated mice and control mice and numerous bacteria were observed in both groups of mice (Fig. 4B, c–f).

$CD4^+CD25^+$ T cells do not suppress protection induced by $CD4^+CD25^-$ T cells against M. tuberculosis infection in reconstituted mice

To further evaluate the role of $CD4^+CD25^+$ Treg cells in mycobacterial infection at late stage (after developing acquired immunity), the following experiment was conducted. $CD4^+CD25^-$ T cells and $CD4^+CD25^+$ T cells were purified from chronically BCG-infected mice: >90% of the $CD4^+CD25^+$ T cells obtained expressed FoxP3 as estimated by FACScan (data not shown). Each T cell subset, either alone or in combination, was then transferred into SCID mice and mice were infected with *M. tuberculosis* Erdman by airborne exposure. Three weeks post-infection, the bacterial number in lungs (Fig. 5A) and survival kinetics of mice (Fig. 5B) were analyzed.

Observed increases in *M. tuberculosis* were similar in both naive SCID mice and SCID mice reconstituted with $CD4^+CD25^+$ T cells alone, suggesting that $CD4^+CD25^+$ T cells offer no protection against *M. tuberculosis*. In contrast, SCID mice reconstituted with $CD4^+CD25^-$ T cells controlled *M. tuberculosis* infection, at a similar level to that of mice reconstituted with the combination of $CD4^+CD25^-$ T cells and $CD4^+CD25^+$ T cells (Fig. 5A). The survival kinetics showed similar outcomes between mice reconstituted with $CD4^+CD25^-$ T cells plus $CD4^+CD25^+$ T cells and $CD4^+CD25^-$ effector T cells alone (Fig. 5B). These data suggest that the role of $CD4^+CD25^+$ Treg cells in host protection is marginal against *M. tuberculosis* in the overall course of infection (Fig. 5B).

Stimulation with mycobacterial antigens fails to express the function of $CD4^+CD25^+$ Treg cells in vitro

To ascertain why $CD4^+CD25^+$ Treg cells have only a minor role in the late stage of mycobacterial infection, we compared the action of $CD4^+CD25^+$ T cells to $CD4^+CD25^-$ T cells *in vitro*. $CD4^+CD25^+$ and $CD4^+CD25^-$ T cells were isolated from normal mice or mice chronically infected with BCG or *M. tuberculosis* and stimulated with PPD or anti-CD3 mAb in the presence of APCs. $CD4^+CD25^+$ T cells alone showed characteristics of Treg cells, which neither proliferate nor produce cytokines in response to neither PPD nor anti-CD3 mAb (Fig. 6, A–J and a–e). Culture experiments using a combination of $CD4^+CD25^+$ and $CD4^+CD25^-$ T cells showed that $CD4^+CD25^+$ T cells derived from both normal and infected mice suppressed proliferation of $CD4^+CD25^-$ T cells and production of cytokines, such as IFN-gamma and IL-10, in a dose-dependent manner following stimulation with anti-CD3 mAb, showing the characteristics in Treg cells. However, following stimulation with PPD, $CD4^+CD25^+$ T cells failed to suppress both proliferation and production of cytokines. In contrast, IL-2 production was suppressed in a dose-dependent manner in the presence of PPD. Definitive IL-6 production was observed when $CD4^+CD25^-$ T cells were incubated alone or combination with $CD4^+CD25^+$ T cells in the presence of PPD (Fig. 6, I, J and e).

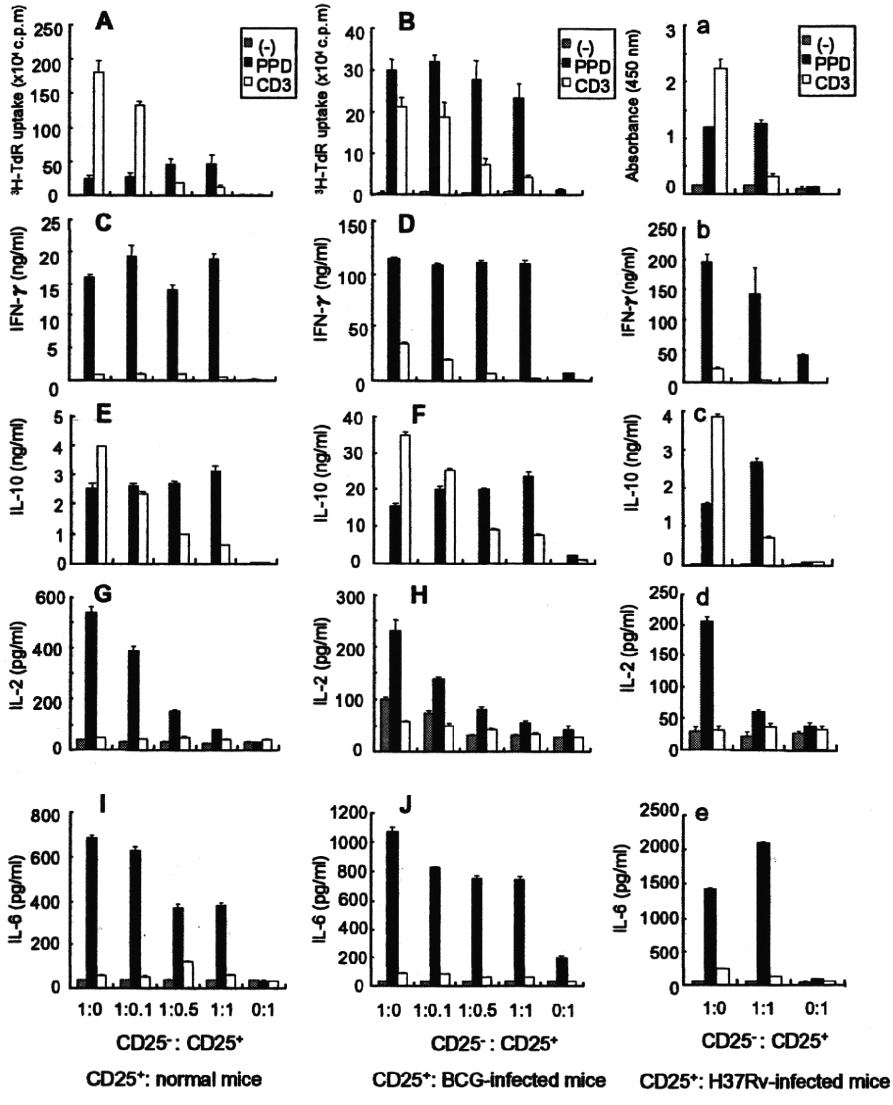

Fig. 6. Stimulation of $CD4^+CD25^+$ T cells by PPD fails to suppress the function of PPD-activated $CD4^+CD25^-$ T cells. $CD4^+CD25^+$ T cells ($CD25^+$) purified from normal (A, C, E, G and I) mice or mice chronically infected with BCG (B, D, F, H and J) or *Mycobacterium tuberculosis* (a–e) were co-cultured with $CD4^+CD25^-$ effector T cells ($CD25^-$) purified from mice chronically infected with BCG or *M. tuberculosis* at various ratios with T cell-depleted irradiated spleen cells (APCs) in the presence of PPD (PPD), or anti-CD3 mAb (CD3), or alone (–). Proliferative responses were analyzed at day 5 (A, B and a). Cytokine production in culture supernatants was measured at day 7 (C, E, I, J and b–e) or day 5 (D, F, G and H).

Soluble mediators are not suppressive factors of $CD4^+CD25^+$ Treg cell function when stimulated with PPD

Because IL-6 allows effector T cells to overcome suppression by $CD4^+CD25^+$ Treg cells (27), we considered the possibility that IL-6 inhibits the function of $CD4^+CD25^+$ Treg cells when stimulated with *M. tuberculosis*-derived mycobacterial antigen, PPD. Therefore, we neutralized IL-6 by neutralizing mAb; however, neutralization of IL-6 did not recover suppressive activity of $CD4^+CD25^+$ Treg cells (Fig. 7A and B).

To determine whether soluble factors beside IL-6 abrogate the suppressive function of $CD4^+CD25^+$ Treg cells upon PPD stimulation, we examined the effects of soluble factors released from T cells and APCs. The culture supernatants from $CD4^+CD25^+$ T cells cultured with both $CD4^+CD25^-$ T cells and APCs in the presence of PPD or anti-CD3 mAb were collected and then transferred to fresh culture of $CD4^+CD25^-$ T cells, $CD4^+CD25^+$ T cells and APCs in the presence or absence of anti-CD3 mAb. The proliferative response of $CD4^+CD25^-$ effector T cells was analyzed by incorporation of [^{3}H]TdR. The results showed that the supernatants of combined $CD4^+CD25^-$ and $CD4^+CD25^+$ T cell culture failed to diminish suppressive activity of proliferative response of $CD4^+CD25^-$ T cells by $CD4^+CD25^+$ T cell stimulated with anti-CD3 mAb (Fig. 8). These results show

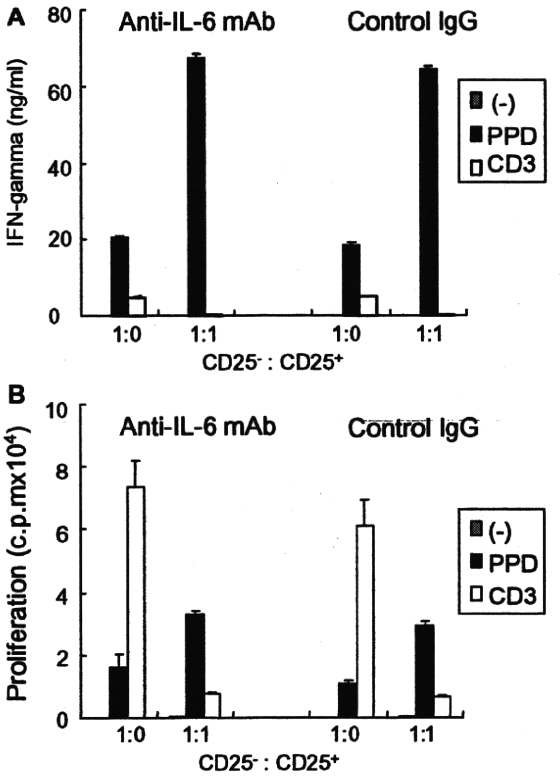

Fig. 7. Neutralization of IL-6 does not affect the $CD4^+CD25^+$ T cell-mediated suppression of the function of effector T cells. $CD4^+CD25^-$ T cells and $CD4^+CD25^+$ T cells were isolated from mice chronically infected with BCG. $CD4^+CD25^-$ effector T cells alone (1:0) or combination of $CD4^+CD25^-$ effector T cells and $CD4^+CD25^+$ T cells (1:1) were cultured with APCs in the presence of PPD (PPD), anti-CD3 mAb (CD3) or absence of these (−). In each well, 0.02 μg ml^{-1} of anti-IL-6 mAb or control IgG were added. IFN-gamma production in culture supernatant (A) and proliferative responses of T cells (B) were analyzed at day 4.

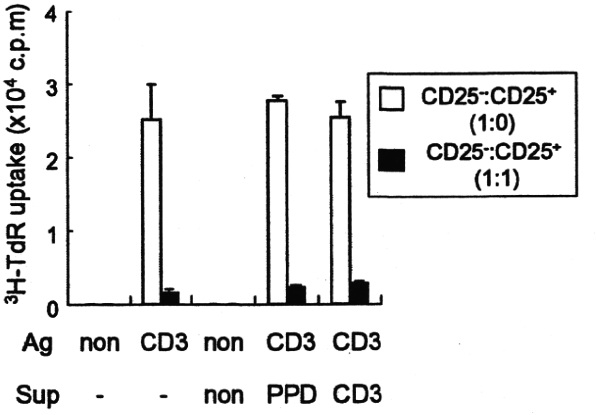

Fig. 8. Soluble mediators upon PPD stimulation do not abrogate $CD4^+CD25^+$ T cell-mediated suppression. $CD4^+CD25^-$ effector T cells ($CD25^-$) and $CD4^+CD25^+$ T cells ($CD25^+$) were isolated from spleens of chronically BCG-infected mice. $CD4^+CD25^-$ T cells/$CD4^+CD25^+$ T cells/APC (1:0:0.1) or $CD4^+CD25^-$ T cells/$CD4^+CD25^+$ cells/APC (1:1:0.1) were cultured with PPD (Sup, PPD), anti-CD3 mAb (Sup, CD3) or alone (Sup, non), for 7 days. Each culture supernatant was stored. Freshly isolated $CD4^+CD25^-$ T cells/$CD4^+CD25^+$ cells/APC (1:0:0.1) or $CD4^+CD25^-$ T cells/$CD4^+CD25^+$ cells/APC (1:1:0.1) were cultured 1:1stored supernatant: fresh culture medium in the presence (Ag, CD3) or absence (Ag, non) of anti-CD3 mAb. Proliferative responses were analyzed at day 4.

that the defective function of $CD4^+CD25^+$ Treg cells following PPD stimulation was not dependent on soluble factors released from T cells and APCs.

Activated $CD4^+CD25^+$ Treg cells suppress the function of PPD-stimulated $CD4^+CD25^-$ effector T cells

Two possibilities could explain the lack of effect of PPD-stimulated $CD4^+CD25^+$ Treg cells on the function of $CD4^+CD25^-$ T cells. First, that activated $CD4^+CD25^+$ Treg cells fail to suppress the function of $CD4^+CD25^-$ T cells by mycobacterial antigens, and second that $CD4^+CD25^+$ Treg cells are not activated by mycobacterial antigens at the late stage of infection. To investigate these possibilities, we purified $CD4^+CD25^+$ T cells from chronically infected mice with BCG or *M. tuberculosis*, then activated *in vitro* with anti-CD3/CD28 mAb-coated beads in the presence of recombinant IL-2. The cells were then cultured with $CD4^+CD25^-$ T cells derived from BCG- or *M. tuberculosis*-infected mice in the presence of PPD. We found that activated $CD4^+CD25^+$ T cells unequivocally suppressed both proliferation and production of IFN-gamma of $CD4^+CD25^-$ T cells stimulated with PPD (Figs 9 and 10). Thus, our data show that both BCG and *M. tuberculosis* infection activate antigen-specific $CD4^+CD25^-$ effector T cells, but not $CD4^+CD25^+$ Treg cells, at the late stage of infection.

Discussion

$CD4^+CD25^+$ Treg cells play a pivotal role in self-tolerance and autoimmune diseases and also in the progression of infectious diseases. It has been shown that $CD4^+CD25^+$ Treg cells are preventive against eradication of persistent pathogens, such as *Leishmania* protozoa, herpes simplex virus and HIV (17–20). Mycobacteria are major parasitic bacteria for eukaryotes (28). In this study, we investigated the role of $CD4^+CD25^+$ Treg cells in mycobacteria infection in mice.

We first studied the effects of Treg cell depletion against infection of mycobacteria. At the early stage of infection, depletion of $CD25^+$ cells significantly suppressed the growth of virulent *M. tuberculosis* strains, such as Kurono and Erdman, suggesting a role for $CD4^+CD25^+$ Treg cells in exacerbation of tuberculosis at the early stage of infection. This is consistent with the previous study performed by Kursar *et al.* (22). This effect of $CD4^+CD25^+$ Treg cells is presumably mediated through naturally occurring $CD4^+CD25^+$ Treg cells, which can be activated through Toll-like receptor (TLR)-mediated signaling (29–32). Mycobacterial DNA [TLR9 ligand (33)] and lipoproteins [TLR2 ligand (34)] may participate in activation of naturally occurring $CD4^+CD25^+$ Treg cells at this stage.

Two to three weeks post-infection, acquired immunity is evident (35). IFN-gamma producing T-helper 1 cells (T_h1) are major effectors in suppressing intracellular survival of

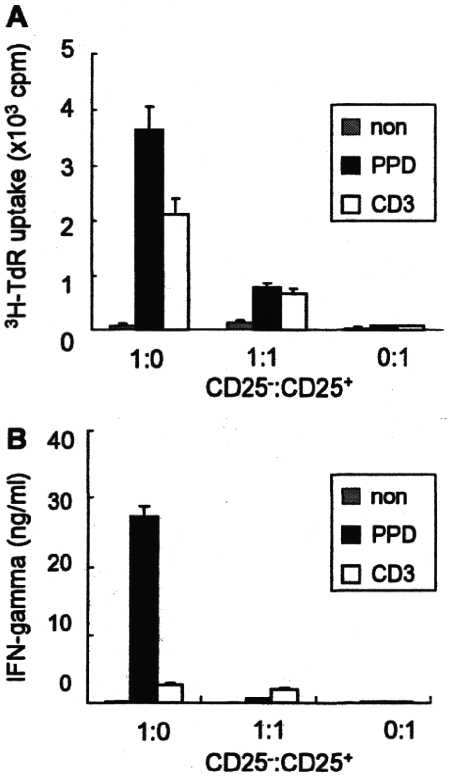

Fig. 9. *In vitro* activation of CD4$^+$CD25$^+$ T cells derived from BCG-infected mice inhibits the function of PPD-stimulated CD4$^+$CD25$^-$ effector T cells. CD4$^+$CD25$^+$ T cells obtained from chronically BCG-infected mice were activated by incubation with anti-CD3/CD28 mAb-coated beads at a bead:cell ratio 2:1 in the presence of 2000 U ml^{-1} of recombinant mouse IL-2 for 48 h. Activated CD4$^+$CD25$^+$ T cells were co-cultured with freshly isolated CD4$^+$CD25$^-$ effector T cells in the presence of PPD (filled column), anti-CD3 mAb (open column) or alone (gray column). (A) Proliferation of CD4$^+$CD25$^-$ effector T cells wase analyzed at day 4. (B) IFN-gamma production in the culture supernatant as measured at day 7.

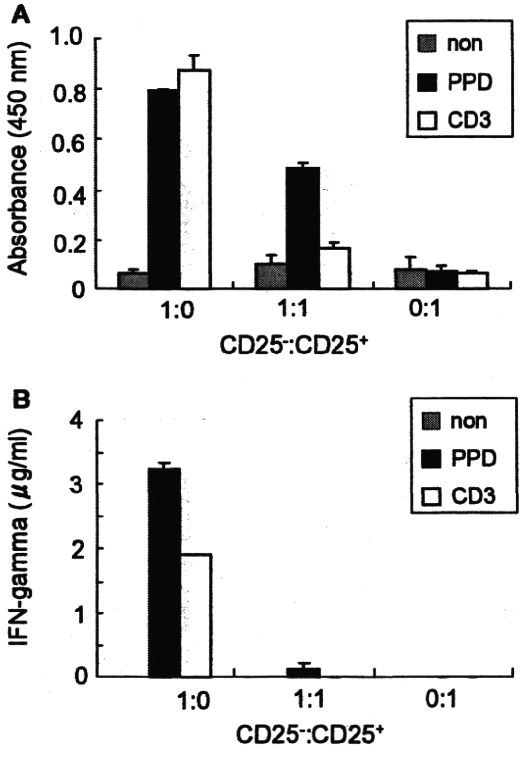

Fig. 10. *In vitro* activation of CD4$^+$CD25$^+$ T cells derived from *Mycobacterium tuberculosis*-infected mice inhibit the function of PPD-stimulated CD4$^+$CD25$^-$ effector T cells. CD4$^+$CD25$^+$ T cells obtained from chronically *M. tuberculosis* H37Rv-infected mice were activated by incubation with anti-CD3/CD28 mAb-coated beads at a bead:cell ratio of 2:1 in the presence of 2000 U ml^{-1} of recombinant mouse IL-2 for 48 h. Activated CD4$^+$CD25$^+$ T cells were co-cultured with freshly isolated CD4$^+$CD25$^-$ effector T cells in the presence of PPD (filled column), anti-CD3 mAb (open column) or alone (gray column). (A) Proliferation of CD4$^+$CD25$^-$ effector T cells was analyzed at day 4. (B) IFN-gamma production in the culture supernatant as measured at day 7.

mycobacteria (36–38). In the CD25$^+$ cell-depletion experiments, the advantages of CD25$^+$ cell depletion were diminished 3 and 5 weeks after the challenge of *M. tuberculosis* Erdman and Kurono, respectively (Figs 2 and 3). We also found that persistence of BCG in mice is not altered by depletion of CD25$^+$ cells by 7D4 (data not shown). These data can be explained by the short-action profile of antibodies. However, we could not find any effect of depletion of CD25$^+$ cells at the chronic stage of infection (Fig. 4), when bacterial numbers were sustained at the same level (39). Similar results were obtained using another anti-CD25 mAb PC6C1, which causes significant reduction of the number of persistent *Leishmania major* in mice by suppressing CD4$^+$CD25$^+$ Treg cells (personal communication with Dr Alan Sher). Furthermore, our *in vivo* experiments in reconstituted SCID mice further suggest that the role of CD4$^+$CD25$^+$ Treg is minimal after infection is established (Fig. 5). The survival kinetics of mice reconstituted with CD4$^+$CD25$^-$ T cells alone are comparable to those in mice reconstituted with both CD4$^+$CD25$^-$ effector T cells and CD4$^+$CD25$^+$ Treg cells (10:1). These data indicate that CD4$^+$CD25$^+$ Treg cells have no impact on the overall outcome of *M. tuberculosis* infection. Kursar *et al.* suggested that CD4$^+$CD25$^+$ Treg cells prevent the bactericidal immune response based on data analyzed in RAG-KO mice reconstituted with each T cell subset (22). However, they reconstituted mice with T cells from naive animals at an unphysiological ratio of CD4$^+$CD25$^-$ T cells to CD4$^+$CD25$^+$ T cells (2:1). These differences may explain the discrepancy between studies.

In order to elucidate the cellular mechanisms of the minimal effect of CD4$^+$CD25$^+$ Treg cells in *M. tuberculosis* infection after the infection was established, we evaluated the function of CD4$^+$CD25$^+$ Treg cells *in vitro*. We activated each population of CD4$^+$ T cells derived from naive and BCG- or *M. tuberculosis*-chronically infected mice with anti-CD3 mAb or *M. tuberculosis*-derived antigens, PPD. BCG has >99.5% identical genome with that of *M. tuberculosis* (40) and therefore BCG and *M. tuberculosis* share almost identical antigens. CD4$^+$CD25$^+$ T cells suppressed anti-CD3-induced

activation (proliferation, production of IFN-gamma and IL-10) of $CD4^+CD25^-$ effector T cells whereas, reflecting our *in vivo* data, PPD stimulation failed to suppress the function of $CD4^+CD25^-$ effector T cells. Both $CD4^+CD25^-$ and $CD4^+CD25^+$ T cells consume IL-2 to proliferate or maintain the state but only $CD25^+CD25^-$ effector T cells produce IL-2. Thus, the level of IL-2 inversely correlated with the number of $CD4^+CD25^+$ T cells (Fig. 6G, H and d) is considered the results of consumption of IL-2 by $CD4^+CD25^+$ T cells but not functional suppression.

One of mechanisms of diminished Treg cell function is mediated by IL-6, which is produced by activated APC through TCR signaling (27). We observed obvious production of IL-6 with PPD stimulation, although which cells produced IL-6 was unknown (Fig. 6, I, J and e). However, neither IL-6 nor other soluble factors released from cells were involved in the non-functional property of $CD4^+CD25^+$ Treg cells following PPD stimulation (Fig. 8). An explanation for this phenomenon is that PPD-specific $CD4^+CD25^+$ Treg cells are not activated at the late stage of mycobacterial infection because $CD4^+CD25^+$ Treg cells activated by anti-CD3/CD28 suppress the function of $CD4^+CD25^-$ effector T cells following stimulation with PPD (Figs 9 and 10).

With the exception of one recent study on herpes simplex virus infection (41), $CD4^+CD25^+$ Treg cells are thought to support parasite persistence in the host by inhibiting the function of effector T cells by a variety of mechanisms. According to this theory, several reports regarding mycobacterial infection have suggested a role for $CD4^+CD25^+$ Treg cells in disease progression and establishment of latent infection (22, 25, 42). However, our findings refute this theory, because $CD4^+CD25^+$ cells did not affect the total infectious load of *M. tuberculosis* in mice (Fig. 5) and mycobacterial infection did not activate mycobacteria-specific $CD4^+CD25^+$ Treg cells (Figs 6, 9 and 10). Several reports showed that FoxP3-positive Treg cells are found in the site of infection with BCG or *M. tuberculosis* (23, 25, 42). However, we consider that these Treg cells are unresponsive to mycobacterial antigens, rather than responding to self-antigens in the disrupted tissues of the infectious legion (43).

In contrast, $CD4^+CD25^+$ Treg cells responding to parasite antigens are activated during infection of *Leishmania* (17, 44) and *Plasmodium* (21). These parasites more closely resemble mammals in the history of evolution; therefore, it can be speculated that they express antigens similar to mammalian self-antigens, which leads to activation of self-antigen-reactive $CD4^+CD25^+$ Treg cells (43). This may be a possible reason for the discrepancy of the host response to mycobacteria versus protozoa. The host must recognize pathogens to survive and mycobacteria represent major bacterial pathogens for vertebrates. In our study, the fact that effector T cells are activated in response to mycobacterial antigens, while suppressive $CD4^+CD25^+$ Treg cells are comparatively silent, is rational based on the host's need to protect itself from mycobacterial infection.

Funding

Japan Health Sciences Foundation; Ministry of Health, Labour and Welfare (Research on Emerging and Re-emerging Infectious Diseases, Health Sciences Research Grants); Ministry of Education, Culture, Sports, Science and Technology; Osaka City University Urban Research; Biochemical Tokyo Research Foundation, and The United States-Japan Cooperative Medical Science Program Against Tuberculosis Leprosy.

Acknowledgements

We would like to thank Dr Toshiki Tamura and Dr Hidefumi Kojima for their advice and Mr Satoru Iwatani for technical support of FACS analysis. We also thank Dr Saburo Yamamoto and Miss Sara Matsumoto for heartfelt encouragement. The authors have no conflicting financial interests.

References

1 Dye, C., Scheele, S., Dolin, P., Pathania, V. and Raviglione, M. C. 1999. Consensus statement. Global burden of tuberculosis: estimated incidence, prevalence, and mortality by country. WHO Global Surveillance and Monitoring Project. *JAMA* 282:677.
2 Jouanguy, E., Altare, F., Lamhamedi, S. *et al.* 1996. Interferon-gamma-receptor deficiency in an infant with fatal bacille Calmette-Guerin infection. *N. Engl. J. Med.* 335:1956.
3 Newport, M. J., Huxley, C. M., Huston, S. *et al.* 1996. A mutation in the interferon-gamma-receptor gene and susceptibility to mycobacterial infection. *N. Engl. J. Med.* 335:1941.
4 Sakaguchi, S. 2000. Regulatory T cells: key controllers of immunologic self-tolerance. *Cell* 101:455.
5 Sakaguchi, S. 2004. Naturally arising CD4+ regulatory t cells for immunologic self-tolerance and negative control of immune responses. *Annu. Rev. Immunol.* 22:531.
6 Shevach, E. M. 2001. Certified professionals: CD4(+)CD25(+) suppressor T cells. *J. Exp. Med.* 193:F41.
7 Read, S., Malmstrom, V. and Powrie, F. 2000. Cytotoxic T lymphocyte-associated antigen 4 plays an essential role in the function of CD25(+)CD4(+) regulatory cells that control intestinal inflammation. *J. Exp. Med.* 192:295.
8 Takahashi, T., Tagami, T., Yamazaki, S. *et al.* 2000. Immunologic self-tolerance maintained by CD25(+)CD4(+) regulatory T cells constitutively expressing cytotoxic T lymphocyte-associated antigen 4. *J. Exp. Med.* 192:303.
9 Shimizu, J., Yamazaki, S., Takahashi, T., Ishida, Y. and Sakaguchi, S. 2002. Stimulation of CD25(+)CD4(+) regulatory T cells through GITR breaks immunological self-tolerance. *Nat. Immunol.* 3:135.
10 McHugh, R. S., Whitters, M. J., Piccirillo, C. A. *et al.* 2002. CD4(+)CD25(+) immunoregulatory T cells: gene expression analysis reveals a functional role for the glucocorticoid-induced TNF receptor. *Immunity* 16:311.
11 Hori, S., Nomura, T. and Sakaguchi, S. 2003. Control of regulatory T cell development by the transcription factor Foxp3. *Science* 299:1057.
12 Sakaguchi, S., Yamaguchi, T., Nomura, T. and Ono, M. 2008. Regulatory T cells and immune tolerance. *Cell* 133:775.
13 Asseman, C., Mauze, S., Leach, M. W., Coffman, R. L. and Powrie, F. 1999. An essential role for interleukin 10 in the function of regulatory T cells that inhibit intestinal inflammation. *J. Exp. Med.* 190:995.
14 Gorelik, L. and Flavell, R. A. 2000. Abrogation of TGFbeta signaling in T cells leads to spontaneous T cell differentiation and autoimmune disease. *Immunity* 12:171.
15 Takahashi, T., Kuniyasu, Y., Toda, M. *et al.* 1998. Immunologic self-tolerance maintained by CD25+CD4+ naturally anergic and suppressive T cells: induction of autoimmune disease by breaking their anergic/suppressive state. *Int. Immunol.* 10:1969.
16 Thornton, A. M. and Shevach, E. M. 1998. CD4+CD25+ immunoregulatory T cells suppress polyclonal T cell activation *in vitro* by inhibiting interleukin 2 production. *J. Exp. Med.* 188:287.
17 Belkaid, Y., Piccirillo, C. A., Mendez, S., Shevach, E. M. and Sacks, D. L. 2002. CD4+CD25+ regulatory T cells control Leishmania major persistence and immunity. *Nature* 420:502.
18 Suvas, S., Kumaraguru, U., Pack, C. D., Lee, S. and Rouse, B. T. 2003. CD4+CD25+ T cells regulate virus-specific primary and memory CD8+ T cell responses. *J. Exp. Med.* 198:889.

19 Aandahl, E. M., Michaelsson, J., Moretto, W. J., Hecht, F. M. and Nixon, D. F. 2004. Human CD4+ CD25+ regulatory T cells control T-cell responses to human immunodeficiency virus and cytomegalovirus antigens. *J. Virol.* 78:2454.

20 Lundgren, A., Suri-Payer, E., Enarsson, K. *et al.* 2003. Helicobacter pylori-specific $CD4^+$ CD25high regulatory T cells suppress memory T-cell responses to H. pylori in infected individuals CD4 T cell activation by myelin oligodendrocyte glycoprotein is suppressed by adult but not cord blood $CD25^+$ T cells. *Infect. Immun.* 71:1755.

21 Hisaeda, H., Maekawa, Y., Iwakawa, D. *et al.* 2004. Escape of malaria parasites from host immunity requires $CD4^+$ $CD25^+$ regulatory T cells. *Nat. Med.* 10:29.

22 Kursar, M., Koch, M., Mittrucker, H. W. *et al.* 2007. Cutting Edge: regulatory T cells prevent efficient clearance of Mycobacterium tuberculosis. *J. Immunol.* 178:2661.

23 Quinn, K. M., McHugh, R. S., Rich, F. J. *et al.* 2006. Inactivation of CD4+ CD25+ regulatory T cells during early mycobacterial infection increases cytokine production but does not affect pathogen load. *Immunol. Cell Biol.* 84:467.

24 Quinn, K. M., Rich, F. J., Goldsack, L. M. *et al.* 2008. Accelerating the secondary immune response by inactivating CD4(+)CD25(+) T regulatory cells prior to BCG vaccination does not enhance protection against tuberculosis. *Eur. J. Immunol.* 38:695.

25 Scott-Browne, J. P., Shafiani, S., Tucker-Heard, G. *et al.* 2007. Expansion and function of Foxp3-expressing T regulatory cells during tuberculosis. *J. Exp. Med.* 204:2159.

26 Kaneko, H., Yamada, H., Mizuno, S. *et al.* 1999. Role of tumor necrosis factor-alpha in *Mycobacterium*-induced granuloma formation in tumor necrosis factor-alpha-deficient mice. *Lab. Invest.* 79:379.

27 Pasare, C. and Medzhitov, R. 2003. Toll pathway-dependent blockade of CD4+CD25+ T cell-mediated suppression by dendritic cells. *Science* 299:1033.

28 Flynn, J. L. and Chan, J. 2001. Immunology of tuberculosis. *Annu. Rev. Immunol.* 19:93.

29 Caramalho, I., Lopes-Carvalho, T., Ostler, D., Zelenay, S., Haury, M. and Demengeot, J. 2003. Regulatory T cells selectively express toll-like receptors and are activated by lipopolysaccharide. *J. Exp. Med.* 197:403.

30 Crellin, N. K., Garcia, R. V., Hadisfar, O., Allan, S. E., Steiner, T. S. and Levings, M. K. 2005. Human CD4+ T cells express TLR5 and its ligand flagellin enhances the suppressive capacity and expression of FOXP3 in CD4+CD25+ T regulatory cells. *J. Immunol.* 175:8051.

31 Peng, G., Guo, Z., Kiniwa, Y. *et al.* 2005. Toll-like receptor 8-mediated reversal of CD4+ regulatory T cell function. *Science* 309:1380.

32 Sutmuller, R. P., den Brok, M. H., Kramer, M. *et al.* 2006. Toll-like receptor 2 controls expansion and function of regulatory T cells. *J. Clin. Invest.* 116:485.

33 Bafica, A., Scanga, C. A., Feng, C. G., Leifer, C., Cheever, A. and Sher, A. 2005. TLR9 regulates Th1 responses and cooperates with TLR2 in mediating optimal resistance to *Mycobacterium tuberculosis*. *J. Exp. Med.* 202:1715.

34 Thoma-Uszynski, S., Stenger, S., Takeuchi, O. *et al.* 2001. Induction of direct antimicrobial activity through mammalian toll-like receptors. *Science* 291:1544.

35 North, R. J. and Jung, Y. J. 2004. Immunity to tuberculosis. *Annu. Rev. Immunol.* 22:599.

36 Flynn, J. L., Chan, J., Triebold, K. J., Dalton, D. K., Stewart, T. A. and Bloom, B. R. 1993. An essential role for interferon gamma in resistance to *Mycobacterium tuberculosis* infection. *J. Exp. Med.* 178:2249.

37 Cooper, A. M., Dalton, D. K., Stewart, T. A., Griffin, J. P., Russell, D. G. and Orme, I. M. 1993. Disseminated tuberculosis in interferon gamma gene-disrupted mice. *J. Exp. Med.* 178:2243.

38 Scanga, C. A., Mohan, V. P., Yu, K. *et al.* 2000. Depletion of CD4(+) T cells causes reactivation of murine persistent tuberculosis despite continued expression of interferon gamma and nitric oxide synthase 2. *J. Exp. Med.* 192:347.

39 Jung, Y. J., LaCourse, R., Ryan, L. and North, R. J. 2002. Evidence inconsistent with a negative influence of T helper 2 cells on protection afforded by a dominant T helper 1 response against Mycobacterium tuberculosis lung infection in mice. *Infect. Immun.* 70:6436.

40 Behr, M. A., Wilson, M. A., Gill, W. P. *et al.* 1999. Comparative genomics of BCG vaccines by whole-genome DNA microarray. *Science* 284:1520.

41 Lund, J. M., Hsing, L., Pham, T. T. and Rudensky, A. Y. 2008. Coordination of early protective immunity to viral infection by regulatory T cells. *Science* 320:1220.

42 Roberts, T., Beyers, N., Aguirre, A. and Walzl, G. 2007. Immunosuppression during active tuberculosis is characterized by decreased interferon- gamma production and CD25 expression with elevated forkhead box P3, transforming growth factor-beta, and interleukin-4 mRNA levels. *J. Infect. Dis.* 195:870.

43 Nishikawa, H., Kato, T., Tawara, I. *et al.* 2005. Definition of target antigens for naturally occurring CD4(+) CD25(+) regulatory T cells. *J. Exp. Med.* 201:681.

44 Mendez, S., Reckling, S. K., Piccirillo, C. A., Sacks, D. and Belkaid, Y. 2004. Role for CD4(+) CD25(+) regulatory T cells in reactivation of persistent leishmaniasis and control of concomitant immunity. *J. Exp. Med.* 200:201.

THE JOURNAL OF BIOLOGICAL CHEMISTRY VOL. 285, NO. 18, pp. 13326–13336, April 30, 2010

Controlled Expression of Branch-forming Mannosyltransferase Is Critical for Mycobacterial Lipoarabinomannan Biosynthesis[S]

Received for publication, October 21, 2009, and in revised form, February 12, 2010 Published, JBC Papers in Press, March 9, 2010, DOI 10.1074/jbc.M109.077297

Chubert B. C. Sena[‡], Takeshi Fukuda[‡], Kana Miyanagi[‡], Sohkichi Matsumoto[§1], Kazuo Kobayashi[¶1], Yoshiko Murakami[‡], Yusuke Maeda[‡], Taroh Kinoshita[‡2], and Yasu S. Morita[‡3]

From the [‡]Research Institute for Microbial Diseases and WPI-Immunology Frontier Research Center, Osaka University, Osaka 565-0871, Japan, the [§]Department of Bacteriology, Osaka City University Graduate School of Medicine, Osaka 545-8585, Japan, and the [¶]Department of Immunology, National Institute of Infectious Diseases, Tokyo 162-8640, Japan

Lipomannan (LM) and lipoarabinomannan (LAM) are phosphatidylinositol-anchored glycans present in the mycobacterial cell wall. In *Mycobacterium smegmatis*, the mannan core of LM/LAM constitutes a linear chain of 20–25 α1,6-mannoses elaborated by 8–9 α1,2-monomannose side branches. At least two α1,6-mannosyltransferases mediate the linear mannose chain elongation, and one branching α1,2-mannosyltransferase (encoded by *MSMEG_4247*) transfers monomannose branches. An *MSMEG_4247* deletion mutant accumulates branchless LAM and interestingly fails to accumulate LM, suggesting an unexpected role of mannose branching for LM synthesis or maintenance. To understand the roles of MSMEG_4247-mediated branching more clearly, we analyzed the *MSMEG_4247* deletion mutant in detail. Our study showed that the deletion mutant restored the synthesis of wild-type LM and LAM upon the expression of MSMEG_4247 at wild-type levels. In striking contrast, overexpression of MSMEG_4247 resulted in the accumulation of dwarfed LM/LAM, although monomannose branching was restored. The dwarfed LAM carried a mannan chain less than half the length of wild-type LAM and was elaborated by an arabinan that was about 4 times smaller. Induced overexpression of an elongating α1,6-mannosyltransferase competed with the overexpressed branching enzyme, alleviating the dwarfing effect of the branching enzyme. In wild-type cells, LM and LAM decreased in quantity in the stationary phase, and the expression levels of branching and elongating mannosyltransferases were reduced in concert, presumably to avoid producing abnormal LM/LAM. These data suggest that the coordinated expressions of branching and elongating mannosyltransferases are critical for mannan backbone elongation.

Mycobacterium tuberculosis is an etiologic agent of tuberculosis, an infectious disease that remains a global problem. Glycoconjugates from the mycobacterial cell wall are involved in pathogenesis and immune modulation. In particular, phosphatidylinositol mannosides (PIMs),[4] lipomannan (LM), and lipoarabinomannan (LAM) form a class of glycoconjugates found in all species of mycobacteria, including pathogenic *M. tuberculosis* and saprophytic and experimentally tractable *Mycobacterium smegmatis*, and are known to have potent immunomodulatory activities (1–3). PIMs are anchored to the plasma membrane by a phosphatidylinositol (PI) and carry two or six mannoses, which are directly linked to the 2-OH and 6-OH of the inositol residue (4, 5) (Fig. 1*A*). Monomannose attached to the 2-OH of inositol is further modified by a fatty acid, making triacylated PIMs the major lipid species. The 3-OH of inositol can be further modified by a fatty acid to become a tetra-acylated species (6). LM carries a much longer chain of mannoses. For example, in *M. smegmatis*, 20–25 α1,6-mannose residues were thought to form a linear chain, which is elaborated by 8–9 α1,2-mannose monomer branches (7). A more recent report estimated *M. smegmatis* LM to carry 21–34 mannose residues (8), highlighting even greater heterogeneity of this molecule. LAM is an arabinosylated LM, in which ~70 residues of D-arabinofuranose form arabinan(s) comprising α1,5 linear stretches linked by multiple α1,3 branch points (9, 10). It is not known if a single molecule of LAM carries a single large arabinan moiety or multiple smaller arabinans.

PIMs, LM, and LAM all contain PI as a common lipid core moiety and are thought to be biosynthesized in a sequential order. PIMs are synthesized from a PI by sequential additions of mannoses, resulting in dimannosyl or hexamannosyl PIMs (6, 11–13). PimA and PimB′ mediate the transfers of first two mannoses in a GDP-mannose-dependent manner, and an acyltransferase, encoded by *MSMEG_2934* in *M. smegmatis*, adds one fatty acid onto a mannose residue to produce a dimannosyl species, AcPIM2 (14–16). Then, an additional four mannose residues are transferred onto AcPIM2, producing AcPIM6.

[S] The on-line version of this article (available at http://www.jbc.org) contains supplemental Table S1 and Figs. S1–S5.

[1] Supported by grants from the Ministry of Health, Labor, and Welfare (Research on Emerging and Re-emerging Infectious Diseases), Ministry of Education, Culture, Sports, Science, and Technology, Japan Health Sciences Foundation, and the United States-Japan Cooperative Medical Science Program against Tuberculosis and Leprosy.

[2] Supported by the Knowledge Cluster Initiative of the Ministry of Education, Culture, Sports, Science, and Technology.

[3] Supported by grants from the International Human Frontier Science Program and Japan Society for the Promotion of Science (KAKENHI 20590441).
To whom correspondence should be addressed: Dept. of Immunoregulation, Research Institute for Microbial Diseases, Osaka University, 3-1 Yamada-oka, Suita, Osaka 565-0871, Japan. Tel.: 81-6-6879-8329; Fax: 81-6-6875-5233; E-mail: ymorita@biken.osaka-u.ac.jp.

[4] The abbreviations used are: PIM, phosphatidylinositol mannoside; HPAEC, high performance anion exchange chromatography; HPTLC, high performance thin layer chromatography; LAM, lipoarabinomannan; LM, lipomannan; PI, phosphatidylinositol; Tricine, *N*-[2-hydroxy-1,1-bis(hydroxymethyl)ethyl]glycine.